## REVIEW ARTICLE

# Single crystal growth and properties of iron-chalcogenide superconductors

Jinsheng Wen<sup>1,2,3</sup>, Guangyong Xu<sup>2</sup>, Genda Gu<sup>2</sup>, J. M. Tranquada<sup>2</sup> and R. J. Birgeneau<sup>1,3</sup>

<sup>1</sup>Physics Department, University of California, Berkeley, California 94720, USA

E-mail: jinshengwen@berkeley.edu, jtran@bnl.gov

Abstract. In this review, we present a summary of the results on single crystal growth and characterization of two types of iron-chalcogenide superconductors,  $\operatorname{Fe}_{1+y}\operatorname{Te}_{1-x}\operatorname{Se}_x$  (11), and  $A_x\operatorname{Fe}_{2-y}\operatorname{Se}_2$  ( $A=\operatorname{K}$ , Rb, Cs, Tl, Tl/K, Tl/Rb), using Bridgman, zone-melting, vapor self-transport, and flux techniques. It will be shown that for the 11 system, while static magnetic order around the reciprocal lattice position (0.5,0) competes with superconductivity, spin excitations centered around (0.5,0.5) are closely coupled to the materials' superconductivity; this is made evident by the strong correlation between the spectral weight around (0.5,0.5) and the superconducting volume fraction. The observation of a spin resonance below the superconducting temperature,  $T_c$ , and the magnetic-field dependence of the resonance, emphasize the important role spin excitations play in the superconductivity. Generally, these results illustrate the similarities between the iron-based and cuprate superconductors. In  $A_x\operatorname{Fe}_{2-y}\operatorname{Se}_2$ , superconductivity with  $T_c\sim 30\ \mathrm{K}$  borders an antiferromagnetic insulating phase; this is closer to the behavior observed in the cuprates but differs from that in other iron-based superconductors.

## Contents

Τ	Inti	roduction	3			
2	Crystal growth					
	2.1	Bridgman method	5			
	2.2	Optical zone-melting technique	6			
	2.3	Vapor self-transport and flux method	8			
3	Sup	erconductivity in iron chalcogenides	8			
	3.1	Superconductivity in the 11 system	8			
	3.2	Pressure study on the 11 system	11			

<sup>&</sup>lt;sup>2</sup>Condensed Matter Physics and Materials Science Department, Brookhaven National Laboratory, Upton, New York 11973, USA

 $<sup>^3{\</sup>rm Materials}$ Science Division, Lawrence Berkeley National Laboratory, Berkeley, California 94720, USA

CONTENTS	9
CONTENTS	

	3.3	Doping with $3d$ transition metals into $Fe_{1+y}Te_{1-x}Se_x$	13
	3.4	Superconductivity in $A_x \text{Fe}_{2-y} \text{Se}_2$ ( $A = K$ , Rb, Cs, Tl, Tl/K, Tl/Rb)	13
	3.5	Summary	16
4	Mag	gnetic correlations	16
	4.1	Magnetic order	16
		4.1.1 $\operatorname{Fe}_{1+y}\operatorname{Te}_{1-x}\operatorname{Se}_x$ system	16
		4.1.2 $A_x \operatorname{Fe}_{2-y} \operatorname{Se}_2$ materials	18
	4.2	Spin excitations in $Fe_{1+y}Te_{1-x}Se_x$	18
		4.2.1 Spin dynamics near $(0.5, 0.5)$	18
		4.2.2 Doping dependence	20
	4.3	Summary	22
5	Con	nclusions	23
6	Ack	knowledgements	24

#### 1. Introduction

A superconducting material can conduct electric current with zero-energy loss due to the absence of electrical resistance below its superconducting transition temperature  $T_c$ ; such behavior is clearly of great practical use [1]. On the theoretical side, superconductivity was initially understood with the elegant many-body theory developed by Bardeen, Cooper, and Schrieffer, (BCS theory) [2]; these authors explained the phenomenon of superconductivity on the basis of electron pairs whose interaction is mediated by electron-phonon coupling. In the 1980s, high-temperature superconductivity was discovered in lamellar copper-oxide materials whose  $T_c$  can be above liquid-nitrogen temperature [3, 4]. Here, the electron-phonon coupling as proposed in BCS theory is not sufficient to induce superconductivity at such high temperatures [5, 6]. In these cuprate superconducting materials, superconductivity develops from electronically doping an antiferromagnetic Mott insulating phase with carriers [5–9]. It is thus hoped that one may eventually understand the high- $T_c$  superconductivity in terms of the interplay between magnetism and superconductivity.

Research on high- $T_c$  superconductivity gained new momentum in the year 2008 with the discovery of iron-pnictide superconductors. The initial excitement came with the discovery by Hosono's group of superconductivity in LaFeAsO<sub>1-x</sub>F<sub>x</sub> (labeled 1111, based on the elemental ratios in the chemical formula of the parent material) with  $T_c = 26$  K [10], following an earlier report by the same group of superconductivity in LaFePO<sub>1-x</sub>F<sub>x</sub> with  $T_c \sim 5$  K [11]. The  $T_c$  was soon raised to 43 K, either by replacing La with Sm (SmFeAsO<sub>1-x</sub>F<sub>x</sub>) [12], or by applying pressure [13]. Several 1111 superconductors with  $T_c > 50$  K have been successively reported [14–17], and the current record is 56 K in Gd<sub>1-x</sub>Th<sub>x</sub>FeAsO [17]. Besides the 1111 system, three other families of iron-based superconductors have been discovered, typified by BaFe<sub>2</sub>As<sub>2</sub> (122) [18–21], LiFeAs (111) [22–28], and Fe<sub>1+y</sub>Te<sub>1-x</sub>Se<sub>x</sub> (11) [29–33]. Their crystal structures, illustrated in figure 1, are all tetragonal at room temperature [11, 26, 34–37]. One important common feature is that they are all layered structures, as in the cuprates [5–9].

Extensive research has been carried out to study the magnetic correlations. It is now well established for these materials that long-range antiferromagnetic order is suppressed with doping, while superconductivity appears above a certain doping level [35–56]. While there are a few cases where superconductivity appears suddenly after magnetic order disappears [45], it is more commonly found that magnetic order, either short- or long-ranged, coexists in some fashion with superconductivity over a finite range of doping [44, 46–50, 52, 54]. The fact that superconductivity develops concomitantly with the suppression of antiferromagnetic order in iron-based superconductors [38, 54, 57, 58], a behaviour similar to that in cuprates [5–9], suggests that there could also be a similar connection with the superconductivity. Conceptually, the simplest possibility would involve having the magnetic excitations replace phonons in the electron pairing interaction, and in the iron-based superconductors the finite

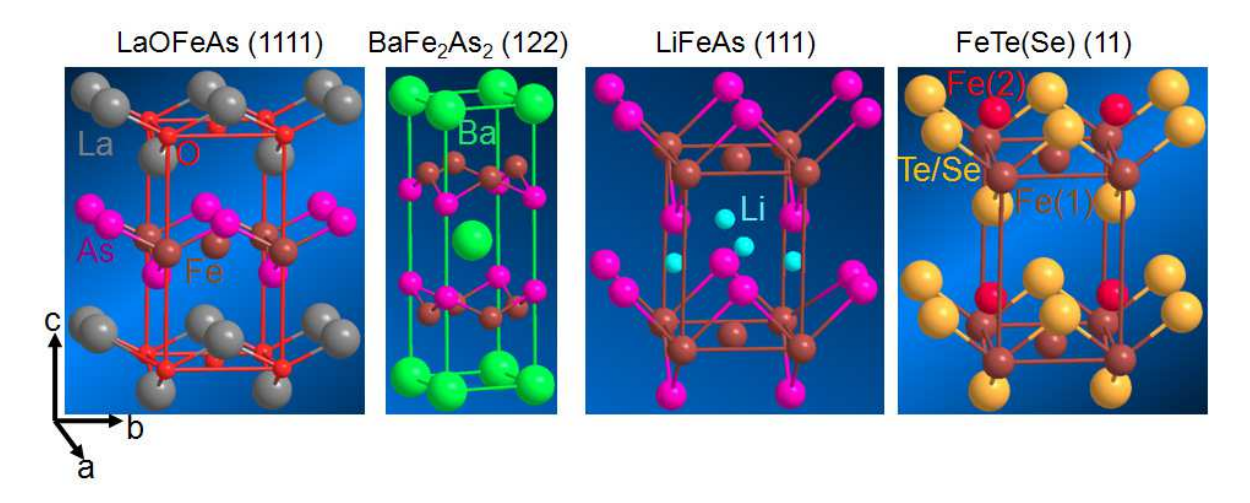


**Figure 1.** Schematic crystal structures for the 1111, 122, 111 and 11 type iron-based superconductors.

momentum of the antiferromagnetic fluctuations is proposed to facilitate interband pairing [59–65]. Of course, the role of the magnetic correlations could depend on the nature of the magnetism, which continues to be a subject of intense investigation [66–73]. Furthermore, four or five Fe 3d orbitals are involved in the multiple bands that cross the Fermi energy, and excitations among these orbitals have also been proposed as possible contributors to the pairing mechanism [74]. In any case, the magnetic excitations respond strongly to the superconductivity: the low-energy fluctuations are gapped, and the spectral weight moves into a "resonance" peak above the gap; the resonance peak has been observed in a number of iron-based superconductors [75–83]. Obviously, the iron-based superconductors provide new opportunities to address the long-standing challenge of high- $T_c$  superconductivity, and this has made them some of the most heavily studied materials in condensed matter physics over the past three years. A number of reviews are already available on these superconductors [55, 84–93].

Among the four types of iron-based superconductors, the  $T_c$  for the 11 system is the lowest [87]. However, the 11 materials are still of particular interest for a number of reasons: i) As seen from figure 1, the crystal structure is the simplest, which makes study easier; ii) It is obvious from the chemical formula that the 11 system is the only one which does not contain As, thus making it safer to handle; iii) Most importantly, high-quality, large-size single crystals are relatively easy to grow for this system, as will be discussed in section 2. This is especially important for neutron scattering experiments because, although neutrons represent a powerful probe of magnetic correlations, the limitations of neutron source strength and scattering cross sections require the use of samples of considerable size ( $\gtrsim 1 \text{ cm}^3$ ) in order to obtain reliable data.

More recently, the discovery of superconductivity in a ternary iron-chalcogenide system with the approximate formula  $A_x$ Fe<sub>2-y</sub>Se<sub>2</sub> (A = K, Rb, Cs, Tl, Tl/K, Tl/Rb), whose highest  $T_c$  is  $\sim 33$  K, has stimulated considerable interest. [94–98] The structure

is equivalent to that of the 122 materials, as shown in figure 1 (122).

The remainder of this paper is organized as follows: in section 2, we present the efforts on crystal growth that make many further measurements possible; in section 3, superconductivity in both the 11 and  $A_x$ Fe<sub>2-y</sub>Se<sub>2</sub> systems is discussed; in section 4, the static and dynamic spin correlations obtained mainly by neutron scattering experiments are presented, followed by the conclusions in section 5.

## 2. Crystal growth

To grow single crystals of  $Fe_{1+y}Te_{1-x}Se_x$  with x < 0.7, several flux-free techniques have been utilized, including Bridgman (vertical and horizontal) [31, 32, 54, 83, 99–110], optical zone-melting [111], and vapor self-transport [112]. For  $Fe_{1+y}Se$ , the phase diagram does not allow self-flux growth, so, instead, growth methods with a NaCl/KCl flux [113] and with a LiCl/CsCl flux [114] have been reported. For the newly discovered  $A_xFe_{2-y}Se_2$  system, typically the Bridgman method has been employed [94–96, 115–119].

## 2.1. Bridgman method

In figure 2(a) and (c) we show the schematics for the vertical and horizontal versions of the Bridgman technique. An example of a synthesis scheme is as follows. To start with, the raw materials (99.999% Te, 99.999% Se, and 99.98% Fe) are weighed and mixed with the desired molar ratio, and then sealed into an evacuated, high-purity (99.995%) quartz tube. Since the tube often cracks during the cooling cycle, it is sealed inside a larger evacuated tube. The doubly-sealed materials are then put into the furnace vertically (or horizontally) for pre-melting, with the following sequence: ramp to 660 °C in 2 hrs; hold for 1 hr; ramp to 900 °C in 1 hr; hold for 1 hr; ramp to 1050 °C in 1 hr; hold for 3 hrs; shut down the furnace and cool to room temperature. The reacted materials are then crushed and double-sealed into evacuated quartz tubes for the growth sequence: ramp to 660 °C in 3 hrs; hold for 1 hr; ramp to 900 °C in 2 hrs; hold for 1 hr; ramp to 1000 °C in 1 hr; hold for 12 hrs; cool to 300 °C with a cooling rate of -0.5 or -1 °C/hr; shut down the furnace and cool to room temperature. In the furnace, there should be a small temperature gradient from one end to the other (e. q., at 850 °C,  $\Delta T$ /distance  $\approx 5$  °C/cm) as shown in figure 2(a) and (c), so that the melted liquid will crystallize unidirectionally. (Some may choose to skip the premelting step.) By using this method, large-size (> 10 g) high-quality single crystals can be obtained for  $Fe_{1+y}Te_{1-x}Se_x$  with x < 0.7. Figure 2(b) and (d) show some of the crystals grown using vertical and horizontal Bridgman methods. The crystals can have nice mirrorlike cleavage surfaces, corresponding to the a-b planes; however, in our experience, such crystals have excess Fe (y > 0) and a reduced superconducting volume fraction. Crystals with a large superconducting volume fraction (with  $y \approx 0$ ) tend to have a textured cleavage surface associated with slight misorientation of grains, due to strain effects that develop on cooling in the constrained cross section of a quartz tube. Many

measurements such as resistivity, magnetization, x-ray diffraction (XRD) and neutron diffraction have been carried out to characterize such crystals and demonstrate their quality [31, 32, 54, 83, 99–110].

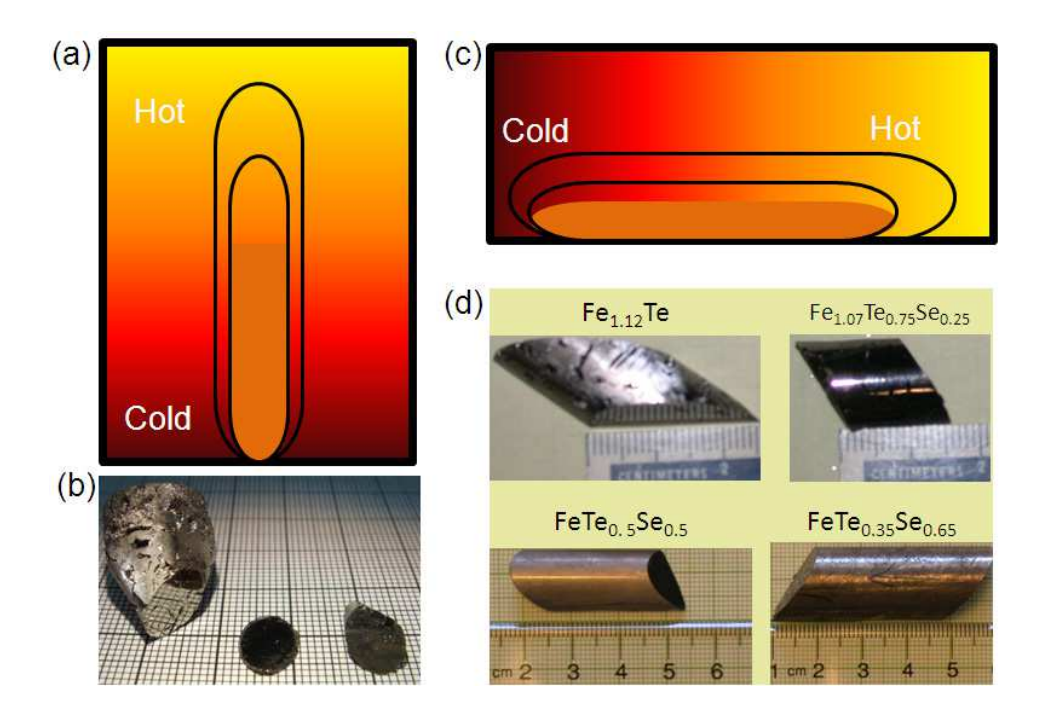


**Figure 2.** (a) Schematic of the vertical Bridgman growth. (b) Crystals grown using the method shown in (a). Reprinted from [31]. © 2009 American Physical Society. (c) Horizontal Bridgman growth. (d) Crystals grown using the method shown in (c) [120].

To grow single crystals of  $A_x$ Fe<sub>2-y</sub>Se<sub>2</sub>, a similar method has been used. First, FeSe is prepared as the precursor by reacting Fe and Se in the appropriate ratio at 700 °C for 4 hrs. The alkali and the precursor FeSe are loaded into an alumina crucible with the nominal composition, which was then sealed into a tube; Wang *et al.* [115] have demonstrated the benefits of using an arc-welded Ta tube. The tube is then put into an evacuated quartz tube and sealed. A typical growth sequence is: ramp to 1050°C in 15 hrs; hold for 4 hrs; cool to 750 °C at a rate of -1 to -3 °C/hr; shut down the furnace and cool to room temperature. Large-size single crystals can be obtained using this method, and single crystal rods so-obtained are shown in figure 3. A one-step method using a similar growth procedure but without first reacting Fe and Se as the precursor has also been reported [119].

## 2.2. Optical zone-melting technique

Yeh et al. [111] have used the optical zone-melting method to grow  $Fe_{1+y}Te_{1-x}Se_x$  single crystals with x ranging from 0 to 0.7. The advantage of this technique is that it offers the possibility of visually examining the locally melted zone, as well as providing convenient control of growth rate using the image furnace. The schematic of the setup is shown



**Figure 3.** Single crystal rods of  $K_{0.8}Fe_2Se_2$  grown using the vertical Bridgman method [121].

in figure 4(a). To grow single crystals, powders of 99.9% Fe, 99.9% Se, and 99.999% Te were combined with the desired stoichiometry and mixed in a ball mill for 4 hrs. The mixed powders were cold pressed into discs under  $400\text{-kg/cm}^2$  uniaxial pressure, and then sealed into an evacuated quartz tube. The tube was heated at 600 °C for 20 hrs. The reacted bulk material was reground to fine powder and then sealed into an evacuated quartz tube. The tube was sealed into a second evacuated tube, and then loaded into an optical floating-zone furnace with two 1500-W halogen lamps installed inside the mirrors as infrared radiation sources, as shown in figure 4(a). The ampule was rotated at a rate of 20 rpm and moved downwards at a rate of 1-2 mm/hr. The as-grown crystals were annealed with the following sequence: ramp to 700-800 °C in 7 hrs; hold for 48 hrs; cool to 420 °C in 4 hrs; hold for 30 hrs; shut down the furnace and cool to room temperature. Figure 4(b) shows an as-grown crystal for FeSe<sub>0.3</sub>Te<sub>0.7</sub>, which has an easily cleaved surface perpendicular the the c axis.

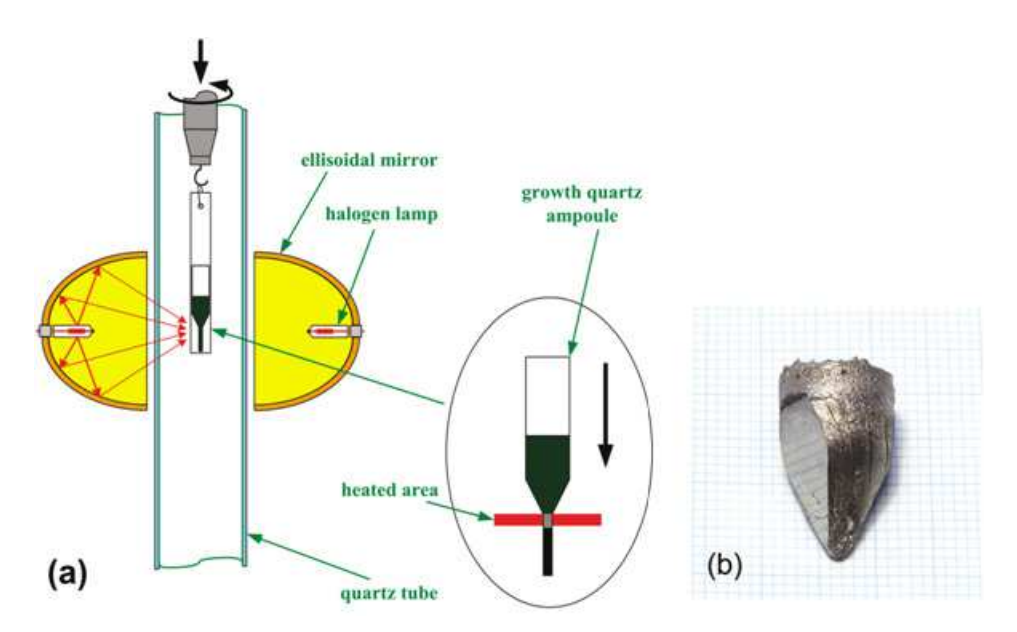


**Figure 4.** (a) Schematic diagram of apparatus setup of the optical zone-melting method. (b) An as-grown FeTe<sub>0.7</sub>Se<sub>0.3</sub> single crystal on a 1-mm grid. The shiny surface is the *a-b* plane. Reprinted from [111]. © 2009 American Chemical Society.

## 2.3. Vapor self-transport and flux method

The phase diagram of Fe-Se is such that one cannot grow large crystals for the  $\beta$ -FeSe directly from self flux; Patel *et al.* [112] used vapor self-transport as an alternative approach. They began by mixing 99.9% Fe and 99.99% Se powders with the desired molar ratio. The mixture was ground and sealed into an evacuated quartz tube. The material was then heated in a three-zone furnace with the following procedure: 1) heat the materials with the temperature for the three zones to be 700 °C, 900 °C, and 900 °C, respectively, for 5 days; 2) crystal nucleation is initiated with a zero-temperature gradient with the temperature of all zones set to 700 °C, and the temperature held constant for 5 hrs; 3) the crystals are left growing for 30 days with a temperature setting of 825 °C, 700 °C, and 825 °C, respectively; 4) the system is cooled to 400 °C rapidly, and the temperature is kept constant for 10 hrs; 5) cool to room temperature at a rate of -3 °C/min. X-ray diffraction indicates that the dominant phase in the as-grown crystal is superconducting  $\beta$ -Fe<sub>1+y</sub>Se, with a minority of non-superconducting  $\beta$ -FeSe [112].

Another approach is to use an alkali-halide flux. Zhang  $et\,al.$  [113] made use of a NaCl/KCl flux. First, Fe and Se powders with the desired stoichiometry were reacted to obtain Fe<sub>1+y</sub>Se polycrystalline samples. This material was mixed with NaCl/KCl flux (ratio 1:1), and the combination was ground and sealed in an evacuated quartz tube. The quartz tube was heated to 850 °C. The temperature was maintained at 850 °C for 2 hrs before cooling to 600 °C at a rate of -3 °C/hr. Finally, the furnace was cooled rapidly to room temperature. The crystals were separated from the flux by dissolving the NaCl/KCl flux in deionized water.

Hu et al. [114] have recently demonstrated an improved method, utilizing a flux of LiCl/CsCl. Refinement of synchrotron x-ray powder diffraction data yielded a stoichiometry of  $Fe_{1.00(2)}Se_{1.00(3)}$ .

## 3. Superconductivity in iron chalcogenides

## 3.1. Superconductivity in the 11 system

Superconductivity in the iron chalcogenides was first discovered in Fe<sub>1+y</sub>Se, with zero resistance at T=8 K, as shown in figure 5 [29]. The upper critical field at zero temperature,  $\mu_0H_{c2}(0)$ , was estimated to be 16.3 T [29]. The crystal structure is the simplest among all iron-based superconductors. At room temperature, Fe<sub>1+y</sub>Se has a tetragonal PbO-type structure belonging to the P4/nmm space group as shown in figure 1(11). It has an iron-based planar sublattice equivalent to that of the iron pnictides [10, 11]. At low temperatures, McQueen et al. [122] found that in a superconducting sample of Fe<sub>1.01</sub>Se there is a transition from a tetragonal to an orthorhombic phase at 90 K. In Fe<sub>1.09</sub>Se, Margadonna et al. [123] observed an orthorhombic phase below 70 K.

Systematic results for the in-plane electrical resistivity of  $Fe_{1+y}Te_{1-x}Se_x$  are shown

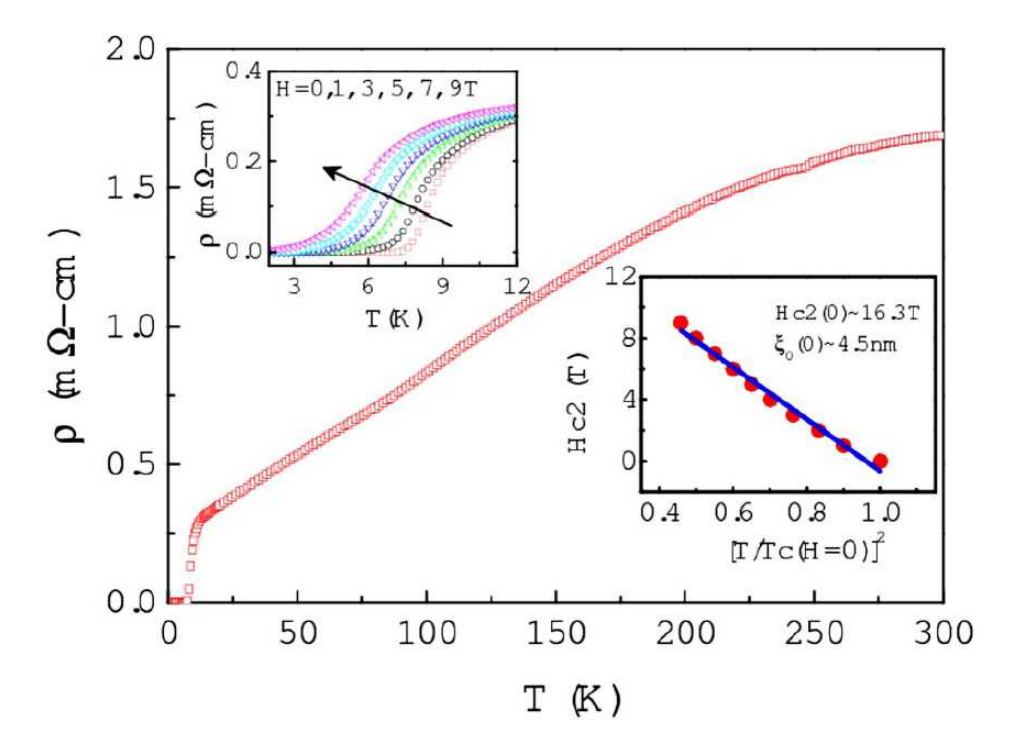
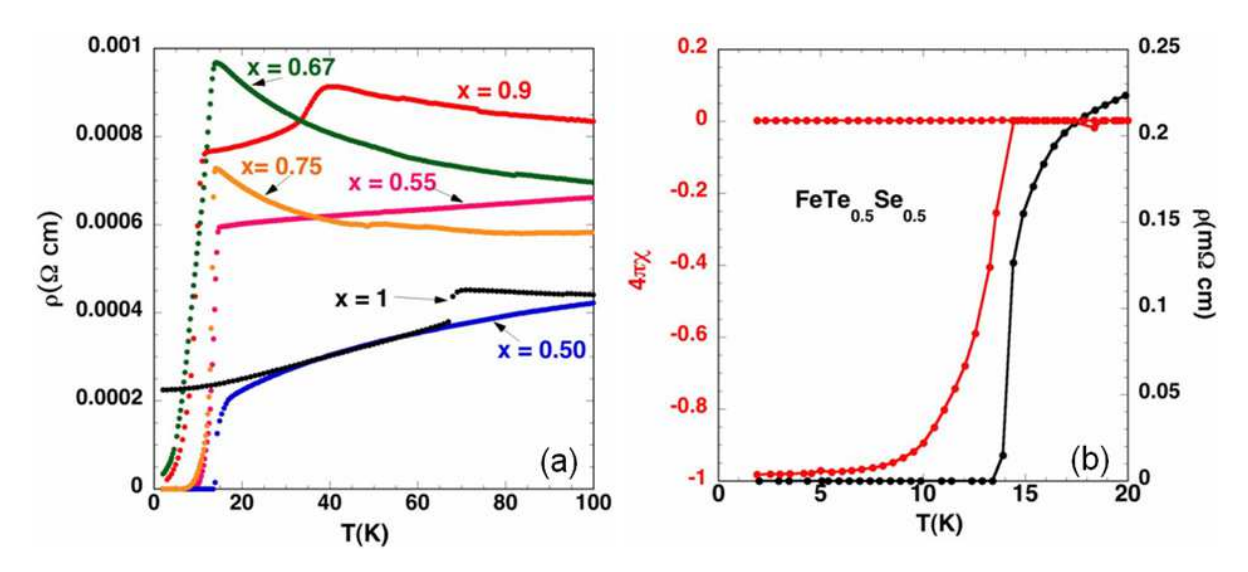


Figure 5. Temperature dependence of electrical resistivity  $(\rho)$  of Fe<sub>1.14</sub>Se. Left inset shows resistivity vs temperature under different field strength below 12 K. Right inset shows the temperature dependence of the upper critical field. Reprinted from [29]. © 2008 National Academy of Sciences of the U.S.A.

in figure 6(a) [31]. Fe<sub>1+y</sub>Te is not superconducting; instead, it exhibits coincident magnetic and structural transitions at  $\sim 65$  K [52, 124–126]. This behaviour is similar to that of the undoped phases of the 1111 and 122 materials [36, 38–56] and the cuprates [5–9], and it is therefore often referred to as the parent compound for the 11 system [33, 124, 125, 127, 128]. By replacing Te with Se, the structural transition temperature is gradually suppressed [129]. With 6% Se doping, a trace of superconductivity starts to appear, and coexists with the antiferromagnetic order [52]. With increasing Se content, the superconducting volume fraction improves, and  $T_c$  also becomes optimized for  $x \sim 0.5$  [30, 31, 33]. Superconductivity extends all of the way to x = 1 in Fe<sub>1+y</sub>Se, as discussed above.

Other combinations of chalcogenides are also possible. For example, one can substitute S for Se in  $Fe_{1+y}Se_{1-z}S_z$ . For z=0.2,  $T_c$  is increased slightly, to 10 K [130]. The  $T_c$  increase is accompanied by suppression of the tetragonal-to-orthorhombic transition temperature, with the transition already absent at z=0.1 [130]. For z>0.2,  $T_c$  gradually decreases, with no superconductivity observed for 40% S [130]. Doping S into the parent compound  $Fe_{1+y}$ Te can also induce superconductivity [99, 110, 127], while suppressing the magnetic and structural transitions. The highest  $T_c$  in the  $Fe_{1+y}$ Te<sub>1-z</sub>S<sub>z</sub> system is 10 K in FeTe<sub>0.8</sub>S<sub>0.2</sub> [127].

Figure 6(b) shows the magnetic susceptibility and resistivity of the optimally-doped



**Figure 6.** (a) In-plane electrical resistivity  $\rho$  as a function of temperature for  $\text{FeTe}_{1-x}\text{Se}_x$ . (b) Magnetic susceptibility of a  $\text{FeTe}_{0.5}\text{Se}_{0.5}$  crystal measured with  $\mu_0H=20$  Oe using zero-field cooling and field-cooling protocols. The resistivity data from the same sample are also shown on the right axis. Reprinted from [31]. © 2008 American Physical Society.

sample, FeTe<sub>0.5</sub>Se<sub>0.5</sub> [31]. It has a  $T_c$  of 14 K, highest in the 11 system under ambient pressure, and the superconducting volume fraction is close to 100% [31, 83]. One thing to note is that in some of the thin film samples, an enhanced  $T_c$  of 17 K was observed [131] (which may be related to strain effects, as pressure can enhance  $T_c$ ; see section 3.2). For this compound, the estimated  $\mu_0 H_{c2}(0)$  is  $\gtrsim 70$  T [83], which makes it comparable with other iron-based and cuprate superconductors [131–133]. Similar to the iron-pnictide superconductors, the anisotropy for the 11 system is small. For instance, in Fe<sub>1.03</sub>Te<sub>0.7</sub>Se<sub>0.3</sub>, the anisotropy coefficient  $\gamma$  (ratio of  $\mu_0 H_{c2}$  measured in and out of plane) is less than 2 [32].

A number of groups have reported similar phase diagrams for  $\text{Fe}_{1+y}\text{Te}_{1-x}\text{Se}_x$  [51–56]; one version, obtained from magnetization measurements, is shown in figure 7. At first glance, this phase diagram is similar to those of the cuprate [5–9] and iron-pnictide superconductors [36, 38–53, 55, 56]. The undoped compound is an antiferromagnet; with doping, the transition temperature is reduced, and superconductivity appears above 0.1 Se doping, with  $T_c$  vs doping x having a dome shape. However, there are several important differences which need to be pointed out: i) Unlike most other high- $T_c$  superconductors, where "doping" refers to substitution of elements with a different valence, here the replacement of Te with Se is isovalent. The positive hall coefficient in  $\text{Fe}_{1.03}\text{Te}_{0.7}\text{Se}_{0.3}$  indicates that hole-carriers are dominant with Se doping [32]; ii) Superconductivity survives to x = 1, unlike most other systems where superconductivity disappears with carrier doping above a certain value [87]; iii) The material's properties can be tuned not only by doping with Se, but also by adjusting the amount of excess Fe. For example,  $\text{F}_{1.01}\text{Se}$  is superconducting with a  $T_c$  of 8 K. With increasing Fe,

 $T_c$  is reduced, and superconductivity is completely suppressed with y = 0.03 [134]. More generally in  $Fe_{1+y}Te_{1-x}Se_x$ , a number of studies have shown that the presence of Fe interstitials correlates with a reduction in superconducting volume fraction [100, 106, 135–137]. Without Se, it appears difficult to reduce Fe content below y = 0.05, but the minimum interstitial density decreases as Se is added [129]. The relationship between excess Fe and the magnetic correlations will be discussed in section 4.

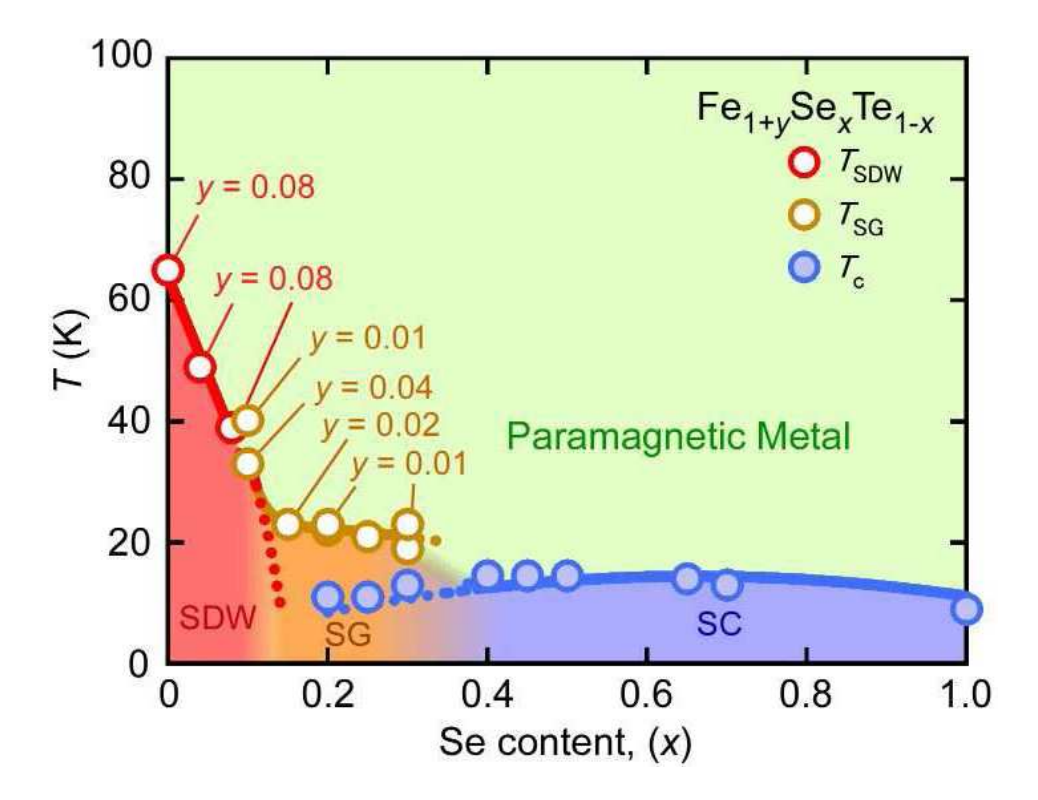


**Figure 7.** Phase diagram of  $Fe_{1+y}Te_{1-x}Se_x$  with y=0 as a function of x and T, constructed from single crystal bulk magnetization data. The nominal Fe content is y=0, unless it is specified. SDW, SG and SC stand for long-range antiferromagnetic, spin-glass and superconducting order respectively. Reprinted from [54]. © 2010 Physical Society of Japan.

#### 3.2. Pressure study on the 11 system

In figure 8 we plot the pressure dependence of  $T_c$  for four samples. For Fe<sub>1+y</sub>Se, there is a strong pressure dependence [138–141]. Applying a pressure of 1.48 GPa raises  $T_c$  to 27 K and  $\mu_0 H_{c2}(0)$  to 72 T [142]. With further increase of pressure,  $T_c$  appears to have a maximum of 37 K for pressures above 4 GPa [138–140]. While  $T_c$  increases with pressure, the superconducting volume fraction is reported to decrease rapidly for pressure (P) > 1.5 GPa, suggesting significant inhomogeneity [143]. Margadonna et al. [139] also found that the  $T_c$ -P curve coincides with anomalies in the pressure evolution of the interlayer spacing, suggesting an intimate relationship between structure and superconductivity.

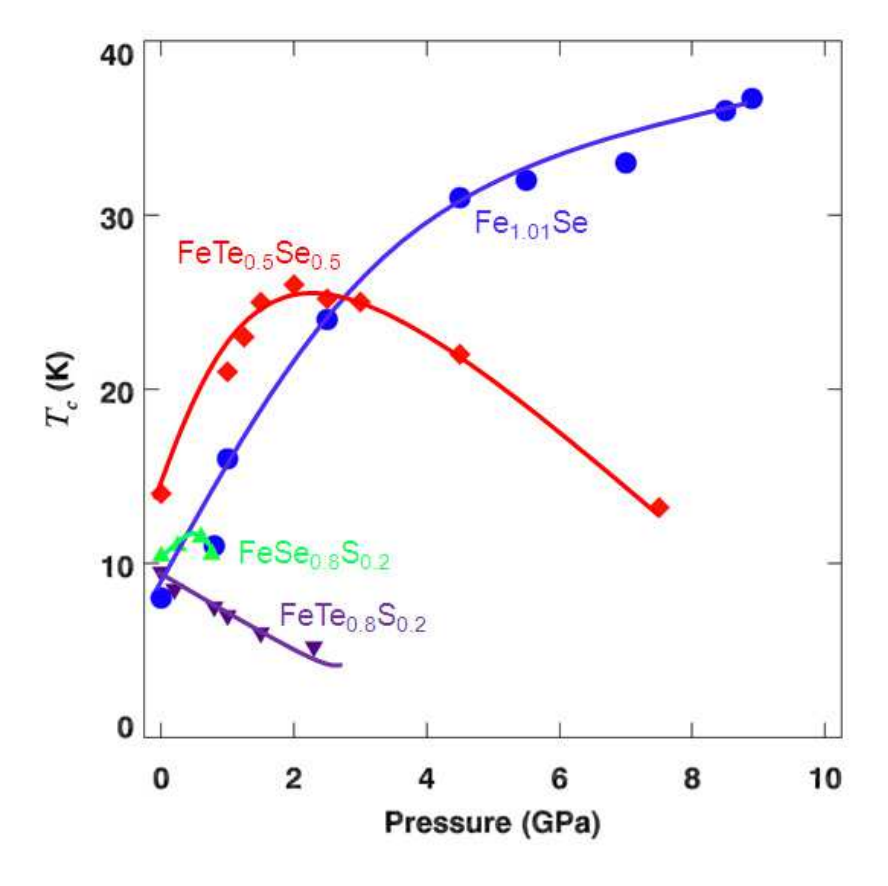


**Figure 8.** Pressure dependence of the  $T_c$  for Fe<sub>1.01</sub>Se, [138] FeTe<sub>0.5</sub>Se<sub>0.5</sub>, [144] FeSe<sub>0.8</sub>S<sub>0.2</sub>, [145] and FeTe<sub>0.8</sub>S<sub>0.2</sub>. [146]

In the compound with mixed Se and Te, the pressure dependence of  $T_c$  is similar to that in Fe<sub>1+y</sub>Se, though less dramatic [144, 145, 147]. In FeTe<sub>0.5</sub>Se<sub>0.5</sub>, the  $T_c$  onset increases rapidly from 13.5 to 26.2 K upon application of a pressure of 2 GPa [144]. Above 2 GPa,  $T_c$  decreases linearly, and a metallic (non-superconducting) ground state is observed at 14 GPa [144]. In other Se-doped samples, e.g., FeTe<sub>0.43</sub>Se<sub>0.57</sub> and FeTe<sub>0.75</sub>Se<sub>0.25</sub>, the pressure effects are reported to be smaller [55, 145, 147].

For FeSe<sub>0.8</sub>S<sub>0.2</sub>, a study with pressure up to 0.76 GPa shows only a weak effect on  $T_c$ , with an indication of a decline in  $T_c$  at higher pressure [145]. Contrary to the pressure enhancement of  $T_c$  discussed so far, application of pressure to Fe<sub>1+y</sub>Te<sub>1-x</sub>S<sub>x</sub> causes  $T_c$  to decrease monotonically, as shown in figure 8 [146]. One might guess that applying pressure to the parent compound of the 11 system, Fe<sub>1+y</sub>Te, could make it superconducting; however, superconductivity was not observed in Fe<sub>1.09</sub>Te with hydrostatic pressure up to 2.5 GPa [148], although the structural transition temperature was reduced [148], and the lattice collapsed [149]. In contrast, superconductivity with  $T_c$  up to 13 K has indeed been reported for thin film samples of FeTe under tensile stress [150].

## 3.3. Doping with 3d transition metals into $Fe_{1+y}Te_{1-x}Se_x$

One can also change the properties of the 11 system by doping with 3d transition metals (Mn, Co, Ni, Cu, etc). There are several initial studies on Fe<sub>1+y</sub>Se [89, 151–153]. Thomas et al. [151] have found that 2.5% Co reduces  $T_c$  to below 4 K, and no superconductivity is observed for Co doping at and above 5%, though the system is sill metallic with 20% Co [130]. Cu seems to have a larger effect in reducing  $T_c$ . As little as 1.5% Cu substitution results in an absence of diamagnetic response [152]. More interestingly, with increased Cu doping (4%), the system evolves into an insulator [152, 153]. Analysis of the temperature dependence of the resistivity suggests that the sample with 10% Cu doping is a Mott insulator [153]. This result has interesting implications for the nature of electronic correlations in the iron chalcogenides. Ni doping is also found to suppress  $T_c$  [130, 154], but does not drive the system to an insulating state for Ni concentations up to 20% [130]. Mn substitution has little effect on  $T_c$ , and the system remains metallic and superconducting with Mn doping up to 5.5% [153].

Similar studies have been carried out in  $Fe_{1+y}Te_{1-x}Se_x$  with x = 0.35 [155] and 0.5 [156]. It is found that Co, Ni, and Cu all suppress  $T_c$  [155], and a metal-to-insulator transition is induced with both Co and Ni doping in  $FeTe_{0.5}Se_{0.5}$  samples [156]. There is also a report on Ni-doped  $Fe_{1.1}Te$ , which reveals that the lattice constants decrease with increasing Ni content [157].

# 3.4. Superconductivity in $A_x Fe_{2-y} Se_2$ (A = K, Rb, Cs, Tl, Tl/K, Tl/Rb)

At the end of the year 2010, Guo et al. [94] reported that superconductivity with  $T_c$  above 30 K had been achieved in a ternary iron chalcogenide,  $K_{0.8}Fe_2Se_2$  by intercalating the metal K in between FeSe layers. In figure 9 we show results for the temperature dependence of the magnetization and in-plane resistivity for a  $K_{0.8}Fe_2Se_2$ single crystal [121]. The  $T_c$  was  $\sim 32.5$  K, the highest among all iron-chalcogenide superconductors at ambient pressure. This new superconductor with such a high  $T_c$  soon ignited another wave of intensive activity. To-date, besides  $K_x Fe_{2-y} Se$  [94, 95, 116, 158– 164, superconductivity has been found in a series of compounds with the formula  $A_x \text{Fe}_{2-y} \text{Se}_2$  where A = Rb, Cs, Tl, Tl/K, or Tl/Rb [96–98, 117, 118, 165–169, 169, 170], and the highest  $T_c$  achieved so far is  $\sim 33$  K. By substituting S ( $K_x Fe_{2-y} Se_{2-z} S_z$ ),  $T_c$ does not decrease for z up to 0.4 [171, 172], but with z = 1.6 superconductivity is completely suppressed [171]. In contrast, Co doping in  $K_{0.8}Fe_2Se_2$  has a very strong effect. With 0.5% Co,  $T_c$  is reduced to 5 K [173]. A number of the newly discovered  $A_x \text{Fe}_{2-y} \text{Se}_2$  superconductors and their  $T_c$ 's are summarized in table 1, from which one can see that the  $T_c$  is not very sensitive to the stoichiometry, except for the Co-doped sample.

There have been some pressure studies on these systems. In a  $K_xFe_2Se_2$  sample, which had a  $T_c$  of 32.6 K,  $T_c$  decreased with increasing pressure, while in a sample with a  $T_c$  of 31.1 K, a dome-shaped  $T_c$ -P curve was observed, with a maximum  $T_c$  of 32.7 K at 0.48 GPa [178]. A similar dome shape was observed for  $Cs_xFe_2Se_2$ , with  $T_c$ 

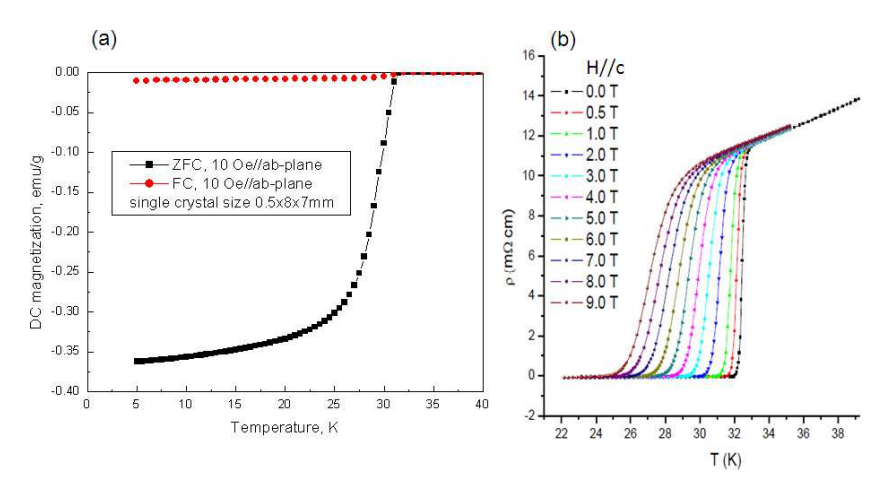


**Figure 9.** (a) Temperature dependence of the magnetization for a  $K_{0.8}Fe_2Se_2$  single crystal. (b) Resistivity measured in the a-b plane with field applied along the c axis [121].

Table 1. Sum	mary of $T_c$ to	or the ne	wly discovered	$1 A_r$ Fe $_2$	."Se₂ su	perconductors.
--------------	------------------	-----------	----------------	-----------------	----------	----------------

Material	$T_c$ (K)	Material	$T_c$ (K)
K <sub>0.8</sub> Fe <sub>2</sub> Se <sub>2</sub> [94, 95, 116, 161, 164, 166]	30-33	$K_{0.8}Fe_2Se_{0.8}S_{1.2}$ [171]	18.2
$K_{0.8}Fe_{1.6}Se_2$ [174]	32	$K_{0.8}Fe_{1.995}Co_{0.005}Se_2$ [173]	5
$K_{0.8}Fe_{1.76}Se_2$ [163]	32	$Rb_{0.8}Fe_2Se_{1.96}$ [165]	31.5
$K_{0.65}Fe_{1.41}Se_2$ [175]	32	$Rb_{0.8}Fe_2Se_2$ [166, 176]	32
$K_{0.85}Fe_{1.83}Se_{2.09}$ [177]	30	$Rb_{0.88}Fe_{1.81}Se_2$ [96]	31.5
$K_{0.85}Fe_2Se_{1.8}$ [178]	32.6	$Cs_{0.86}Fe_{1.66}Se_2$ [117, 166, 178]	30
$K_{0.86}Fe_2Se_{1.82}$ [117, 178]	31.1	$Cs_{0.8}Fe_2Se_{1.96}$ [97, 168, 170]	27 - 28.5
$K_{0.7}Fe_{1.8}Se_2$ [162]	28	$Cs_{0.8}Fe_2Se_2$ [167]	32
$K_{0.86}Fe_{1.73}Se_2$ [160]	25	$TlFe_{1.7}Se_2$ [118]	22.8
$K_{0.86}Fe_{1.84}Se_2$ [159]	30	$Tl_{0.58}K_{0.42}Fe_{1.72}Se_2$ [98, 179]	32
$K_{0.8}Fe_2Se_{1.96}$ [165]	29.5	$Tl_{0.64}K_{0.36}Fe_{1.83}Se_2$ [118]	31
$K_{0.8}Fe_{1.7}SeS$ [180]	25	$Tl_{0.63}K_{0.37}Fe_{1.78}Se_2$ [181]	29
$K_{0.8}Fe_2Se_{1.4}S_{0.4}$ [172]	32.8	$Tl_{0.47}Rb_{0.34}Fe_{1.63}Se_2$ [182]	33
$K_{0.8}Fe_2Se_{1.6}S_{0.4}$ [171]	33.2	$Tl_{0.58}Rb_{0.42}Fe_{1.72}Se_2$ [98]	32
$K_{0.8} \text{Fe}_2 \text{Se}_{1.2} \text{S}_{0.8} [171]$	24.6	$Tl_{0.4}Rb_{0.4}Fe_{2-y}Se_2$ [169]	31.8

maximized to 31.1 K at P=0.82 GPa, compared to 30 K at ambient pressure [178]. In a sample with nominal composition of  $K_{0.8}Fe_2Se_2$ , which had a  $T_c$  of 33 K, it was found that although the onset  $T_c$  increased with pressure, the temperature where the resistivity reached zero decreased [183]. In all of the samples studied, the large normal-state resistance was greatly reduced by pressure [167, 178, 183, 184]. In  $Cs_{0.8}Fe_2Se_2$ , the resistance decreased by two orders of magnitude, concomitant with a sudden  $T_c$  reduction at  $\sim 8$  GPa [167].

In the normal state of these materials, the resistivity-temperature curve exhibits a very pronounced hump [94], which is believed to be irrelevant to superconductivity [115, 166, 178]. However, in  $K_{0.8}Fe_{1.7}Se_2$ , Guo  $et\,al.$  [184] find an interesting correlation between superconductivity and the hump: with increasing pressure, the magnitude of the hump went down as  $T_c$  did, and the hump disappeared at P=9.2 GPa, in coincidence with the complete suppression of the superconductivity. By normalizing the resistance to the room-temperature value, Seyfarth  $et\,al.$  [167] found that the hump still existed at P=9 GPa, at which pressure the sample was not superconductivity. based on this, they concluded that the hump was not related to the superconductivity.

These newly discovered superconductors are particularly interesting and fundamentally important in part due to their electronic structures. First-principle calculations have shown that the band structure in this new system is quite different from that of other iron-based superconductors [185–190]. In particular, the band near the Brillouin zone center  $\Gamma$  point sinks well below the Fermi level [185–190]. Experimentally, this prediction has been verified by several initial angle-resolved photoemission spectroscopy (ARPES) studies, which show that there is no hole pocket near the  $\Gamma$  point [191, 192]. Instead, there are electron pockets near both the  $\Gamma$  and M (Brillouin zone corner) points [179, 181, 193]. Although this result does not rule out the possibility that interband scattering between the electron pockets at  $\Gamma$  and M could be important to the superconductivity [194], the sign-changed  $s_{\pm}$  pairing symmetry which has been suggested in other iron-based superconductors is not likely to apply here [59, 60, 195]. Several alternatives, including d-wave [194, 196], s-wave [197, 198], and  $s_{++}$ -wave [199] superconductivity have been proposed theoretically. A number of ARPES [179, 181, 191–193], nuclear magnetic resonance (NMR) [161, 164, 200], and specific heat measurements [158] have been carried out and all of them indicate that the gap is nodeless.

Another interesting feature which distinguishes the  $A_x$ Fe<sub>2-y</sub>Se<sub>2</sub> superconductors from other iron-based superconductors is that their superconductivity is in close vicinity to an insulating state, similar to the case of cuprate superconductors [5–9], but not to that of other iron-based superconductors [91]. Interestingly, it is reported that the insulating  $K_x$ Fe<sub>2-y</sub>Se sample becomes superconducting by annealing and quenching, and after a few days at room temperature, it is insulating again, showing that the insulating and superconducting states are reversible [201]. Based on these observations, it is suggested that disordering of Fe vacancies plays a key role in rendering the superconductivity [201]. The experimentally observed insulating ground state [118, 166, 171, 180, 202] has stimulated several theoretical calculations [185, 186, 203]. Two possible origins of the insulating behaviour have been proposed which are to be verified experimentally: the system might be a Mott insulator, as in the cuprates [180, 190, 203], or it might be a band insulator resulting from the electronic structure reconstruction due to ordered Fe vacancies [185, 186].

### 3.5. Summary

To summarize this section, it is found that the parent compound for the 11 system,  $\text{Fe}_{1+y}\text{Te}$ , is non-superconducting, and superconductivity is achieved by replacing Te with Se or S. The optimal superconductivity with  $T_c$  of 14 K is found to be in samples with y=0 and  $x\approx 0.5$ .  $\text{Fe}_{1+y}\text{Se}$  is where superconductivity was initially discovered for the 11 system; it has a  $T_c$  of 8 K. The  $T_c$  increases to  $\sim 37$  K upon application of hydrostatic pressure. The superconductivity seems to be vulnerable to doping with 3d transition metals, which can tune the system to a (possibly Mott) insulating regime. More recently, a series of ternary iron-chalcogenide compound with the chemical formula  $A_x\text{Fe}_{2-y}\text{Se}$  were found to be superconducting with  $T_c$  up to 33 K, the highest among all Fe-Se-based superconductors at ambient pressure.

## 4. Magnetic correlations

## 4.1. Magnetic order

4.1.1.  $Fe_{1+y}Te_{1-x}Se_x$  system The magnetic order in  $Fe_{1+y}Te_{1-x}Se_x$  has attracted considerable attention because of its rich physics. An initial band-structure calculation predicted that the Fermi-surface topology in this system should be similar to that of the iron prictides [204]; this has been confirmed by ARPES measurements [205, 206]. From the Fermi-surface-nesting picture [204], one would expect that this system has collinear (C-type) spin-density-wave (SDW) order with an in-plane wave vector (0.5, 0.5), assuming a unit cell containing two irons as shown in figure 10(b). However, several decades ago, Fruchart et al. [207] determined that the magnetic ordering vector is (0.5,0) in Fe<sub>1.125</sub>Te. This result has been confirmed by Bao et al. [124] in Fe<sub>1.075</sub>Te, and by Li et al. [125] in Fe<sub>1.068</sub>Te; each of these has a bicollinear (E-type) spin structure as shown in figure 10(a). Even more surprising is the fact that ARPES measurements have observed no SDW nesting instability along (0.5,0), although there is a weak hole pocket around the X point [205, 208]. Clearly, a simple nesting mechanism cannot account for these experimental results. More recent first-principle calculations have identified the role of local-moments and the importance of Hund's exchange coupling, and have provided better agreement with the experimental observations [41, 72, 209–213].

The magnetic order in Fe<sub>1+y</sub>Te is long-ranged, with a maximum moment size of  $\sim 2.5~\mu_{\rm B}/{\rm Fe}$  for y=0.05~[129]; the moment size decreases for larger y~[124,~125,~207]. The moment size is significant compared to that in iron-pnictide antiferromagnets, but it is small compared to the effective moment estimated from the magnetic susceptibility in the paramagnetic phase [214]. The moment is found to be aligned mostly along the b axis as shown in figure 10(a) [124, 125, 129]. Bao et al. [124] have shown that the order can be commensurate or incommensurate depending upon the amount of excess Fe—with more Fe, the incommensurability is larger. Upon doping with Se, the order is suppressed, with a reduced ordering temperature (from 65 to  $\lesssim 30~{\rm K}$  with 0.1 Se) [54], reduced size of the ordered magnetic moment (from 2.1 to 0.27  $\mu_{\rm B}/{\rm Fe}$ ) [52], and shorter correlation length

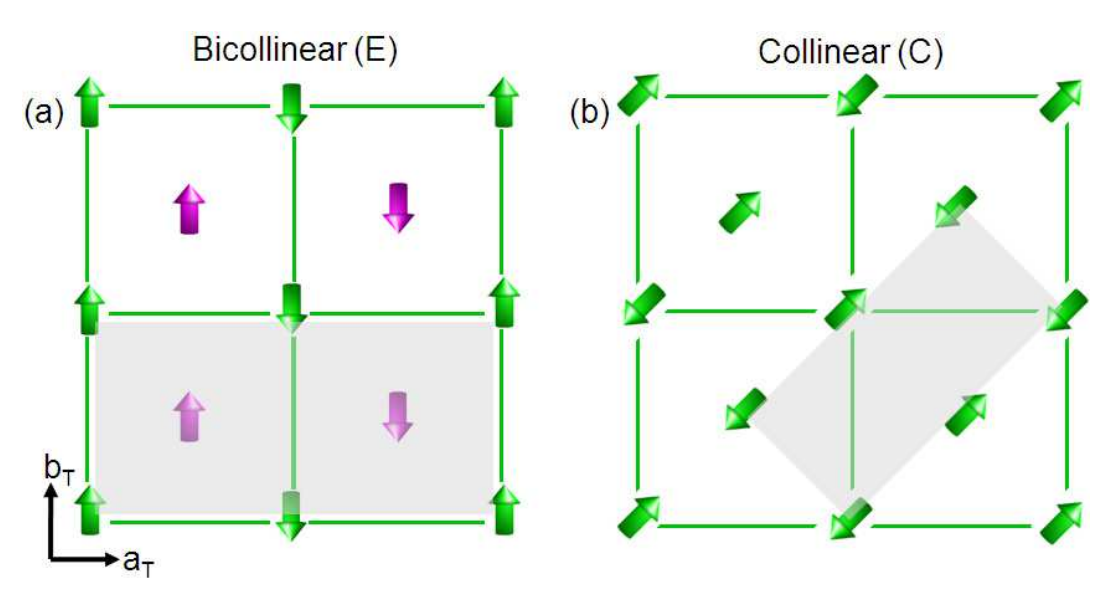


**Figure 10.** (a) Schematic for the bicollinear (E-type) in-plane spin structure in tetragonal notation of the 11 compound. (b) Collinear (C-type) magnetic structure for iron pnictides. Shadow represents the magnetic unit cell.

(the magnetic peak is resolution limited in the parent compound, while with 0.25 Se doping, the order is short-ranged with a correlation length of  $\sim 4$  Å [103, 124]). For Se content above 0.15, there is a phase where spin-glass order and superconductivity coexist [51, 52, 54, 103, 126]. In two single crystal samples,  $Fe_{1.07}Te_{0.75}Se_{0.25}$  and FeTe<sub>0.7</sub>Se<sub>0.3</sub>, both exhibiting short-range incommensurate order below 40 K, it is found that with increasing excess Fe, the incommensurability is larger, similar to the case in the parent compound [103, 124]. In FeTe<sub>0.7</sub>Se<sub>0.3</sub>, which has more Se and less Fe than the Fe<sub>1.07</sub>Te<sub>0.75</sub>Se<sub>0.25</sub> sample, the spin-glass order is depressed, with weaker peak intensity and shorter correlation length, while superconductivity is enhanced, with higher  $T_c$ and superconducting volume fraction [103]. Interestingly, a magnetic peak is only observed on one side of the commensurate wave vector (0.5,0), [i. e.  $(0.5-\delta,0)$  and not  $(0.5\pm\delta,0)$  with  $\delta$  being the incommensurability]; this is likely a result of an imbalance of ferromagnetic/antiferromagnetic correlations between neighbouring spins [103]. (A closely related picture of spin clusters is indicated by a recent study of Fe<sub>1.1</sub>Te [214].) With further increase of the Se concentration, the superconductivity optimizes with  $x \approx 0.5$ , and no static magnetic order is observed (for  $y \sim 0$ ) [51, 52, 83].

On the other end of the phase diagram, there is no static magnetic order in  $\text{Fe}_{1+y}\text{Se}$ , although in some samples these is a symmetry-lowering structural phase transition [122, 134, 138, 215, 216]. In a nuclear magnetic resonance (NMR) study on <sup>77</sup>Se in  $\text{Fe}_{1.01}\text{Se}$  [215], it was found that the spin fluctuations increase on cooling towards  $T_c$ , and they are enhanced under pressure, together with  $T_c$ . It is thus believed that the spin fluctuations are positive for the superconductivity [215]. (The connection between spin fluctuations and superconductivity will be further discussed in section 4.2.) No static magnetic order was detected in a Mössbauer study with P up to 30 GPa [138].

Interestingly, Bendele et al. [216] have reported that  $P \gtrsim 0.8$  GPa will induce short-range magnetic order which coexists with superconductivity, based on muon-spin rotation ( $\mu$ SR) measurements. Mössbauer studies have shown that doping Cu into Fe<sub>1+y</sub>Se induces a local magnetic moment, with the size of the moment increasing with Cu doping while superconductivity is suppressed [152]. Spin-glass behavior has been inferred from magnetization measurements on these Cu-doped samples [152].

The magnetic and superconducting phases in  $Fe_{1+y}Te_{1-x}Se_x$  are summarized in figure 7. Overall, the behaviour is consistent with the common belief that static magnetic order competes with superconductivity, while spin fluctuations promote it.

4.1.2.  $A_x Fe_{2-y} Se_2$  materials Antiferromagnetic order was found in  $TlFe_{2-y} Se_2$  by neutron and Mössbauer measurements [217, 218] long before the recent discovery of superconductivity in the related  $A_x \text{Fe}_{2-y} \text{Se}_2$  compounds. Bao et al. [174] have recently used neutron powder diffraction to determine the crystalline and magnetic structure for  $K_x Fe_{2-x} Se_2$ . At high temperature, the crystal structure is equivalent to that of the 122 materials. At lower temperature, the Fe vacancy order drives the system to an I4/mphase with an enlarged unit cell of  $\sqrt{5} \times \sqrt{5} \times 1$ , which contains a pair of the Fe-Se layers related by inversion symmetry. It is found that  $T_N$  is as high as 559 K and that the magnetic moment is as large as 3.31  $\mu_{\rm B}/{\rm Fe}$ , forming a collinear antiferromagnetic structure with (101) being the propagation wave vector [202]. The moment points mainly along the c axis [174]. It is intriguing that the magnetic order occurs in a tetragonal phase without breaking the four-fold symmetry, although the presence of Fe vacancies may reduce any magnetic frustration [219]. More surprisingly, it has been reported that superconductivity coexists with the strong antiferromagnetic order, both in the neutron study of  $K_{0.8}Fe_2Se_2$  [174] and in the  $\mu SR$  study of  $Cs_{0.8}Fe_2Se_{1.96}$ , [170]. There have been many further observations of the coexistence of superconductivity and antiferromagnetic order [165, 168, 169, 177, 220]. However, due to the difficulty in obtaining samples with high superconducting volume fraction, as well as evidence from transmission electron microscopy for structural inhomogeneity [221], it is not yet clear whether the superconductivity and antiferromagnetic order coexist locally or in different regions of a sample.

## 4.2. Spin excitations in $Fe_{1+y}Te_{1-x}Se_x$

4.2.1. Spin dynamics near (0.5, 0.5) The "resonance" mode in the magnetic excitations, which is defined as the energy at which there is a significant increase in spectral weight when the system enters the superconducting phase, has been the subject of extensive measurements. The resonance is predicted to occur at a particular wave vector if it connects portions of the Fermi surface that have opposite signs of the superconducting gap function. Therefore, observations of the resonance may provide important information relevant to the pairing symmetry [222–225]. (Note that these analyses make the assumption that the magnetism is due to the same electrons that

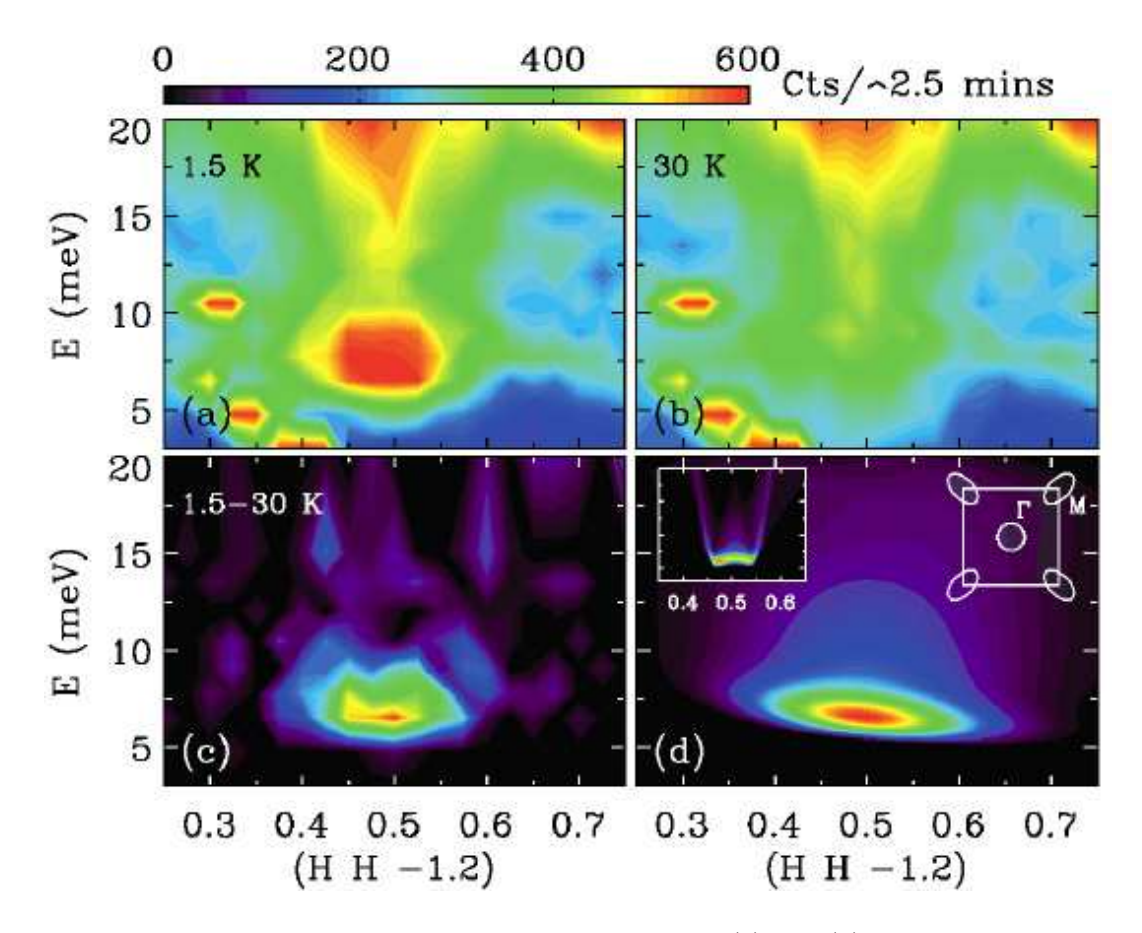


Figure 11. Spin resonance in FeTe<sub>0.6</sub>Se<sub>0.4</sub>. (a) and (b) shows the spin excitation spectrum as a function of **Q** and energy at 1.5 and 30 K respectively. (c) shows the resonance intensity as determined by the difference between the 1.5 and 30 K spectra. (d) Calculated intensity difference from a simplified two-band model with resolution convolved. The left inset shows the resolution-free calculated intensity and the right inset is the normal-state Fermi surface employed in the calculation. Reprinted from [81]. © 2009 American Physical Society.

participate in the superconductivity; further below we will mention reasons to question this assumption.) Resonance excitations have been observed in a number of iron-based superconductors [75, 80], consistent with the presumed gap-sign change between the hole and electron pockets [195]. In Fe<sub>1+y</sub>Te<sub>1-x</sub>Se<sub>x</sub>, despite the fact that the magnetic ordering wave vector is different from that of iron pnictides by 45°, the resonance excitation was observed to be near the same (0.5, 0.5) wave vector by several groups [81–83, 105, 226–228]. Compared to the magnetic excitation spectrum above  $T_c$ , the low-temperature spectral weight is greatly enhanced around (0.5, 0.5) and the resonance energy of ~ 6.5 meV, as shown in figure 11(c) [81]. The resonance energy corresonds to ~  $5k_BT_c$ , similar to the situations in other high- $T_c$  superconductors [87]. Accompanying the resonance, there is a spin gap with an energy of ~ 4 meV; the intensity below the spin gap is shifted to the resonance in the superconducting state [81, 83].

Interestingly, it is found that the resonance is incommensurate in  $\mathbf{Q}$ , peaking at

 $(0.5\pm\delta,0.5\mp\delta)$ , in a direction transverse to (0.5,0.5) [105]. Results on the **Q** dependence of the magnetic response at 6.5 meV are plotted in figure 12. Transverse scans along [110] exhibit a pair of peaks as shown in figure 12(a), while longitudinal scans show a single broad peak centered at (0.5,0.5), as shown in figure 12(b). In both cases, the intensity is enhanced when the sample is cooled below  $T_c$ . The color-coded plot of intensity vs **Q** at 6.5 meV and T=1.5 K, figure 12(c), demonstrates an intriguing anisotropy: the transverse peaks are not reproduced along the longitudinal direction.

For other energies, the anisotropy still persists [82, 226–229], showing that the magnetic excitations are anisotropic, dispersing only along the direction transverse to (0.5, 0.5), as shown in figure 12(d). This is certainly not a spin-wave like excitation, as in CaFe<sub>2</sub>As<sub>2</sub> [230, 231], since in that case one would expect to see a cone-shaped dispersion. ARPES measurements on the sample found that the Fermi surface near (0.5, 0.5) appears to consist of four incommensurate pockets [105]. While Fermi-surface nesting is in principle compatible with the observation of the incommensurate resonance, the dispersion of isolated intensity peaks along a single direction is quite unusual and requires consideration of coupling of spin and orbital effects [105].

Since superconductivity, and hence the pairing, is sensitive to magnetic field, one would naturally expect that an external magnetic field could impact the resonance, as seen in YBa<sub>2</sub>Cu<sub>3</sub>O<sub>6.6</sub> [232] and in La<sub>1.82</sub>Sr<sub>0.18</sub>CuO<sub>4</sub> [233]. Qiu *et al.* [81] found no significant change in the resonance in FeTe<sub>0.6</sub>Se<sub>0.4</sub> in the presence of a 7-T field on a cold-neutron spectrometer with low flux. Another experiment on FeTe<sub>0.5</sub>Se<sub>0.5</sub> using a spectrometer with higher flux concluded that the resonance starts to appear at a lowered  $T_c$ , 12 K, with reduced intensity, due to the suppression of the superconductivity; however, there was no detectable change in either the resonance energy or the width of the resonance peak [83]. With a field of 14.5 T, Zhao *et al.* [234] have shown that in BaFe<sub>1.9</sub>Ni<sub>0.1</sub>As<sub>2</sub>, both the resonance energy and intensity are reduced, and the resonance peak is slightly broadened.

One commonly adopted view is that the spin resonance is a singlet-to-triplet excitation [224, 225, 235]. In principle, this hypothesis can be tested by experiments in magnetic field which should induce Zeeman splitting and lift the degeneracy of the triplet excited state [232]. Bao *et al.* [236] tried to address this problem by applying a 14-T field on FeSe<sub>0.4</sub>Te<sub>0.6</sub>, and it appears that the field induces a peak splitting, which may be in support of this idea.

4.2.2. Doping dependence As discussed above, the non-superconducting parent compound of the 11 system,  $Fe_{1+y}$ Te, has static magnetic order with a bicollinear spin configuration. In samples with good superconducting properties, there is strong magnetic scattering around (0.5, 0.5) with a spin resonance below  $T_c$ , corresponding to spin correlations of the collinear type. A number of theoretical [212, 237] and experimental [52, 106, 228, 229] studies have been carried out on the doping evolution of the magnetic correlations (static and dynamic), and their correlation with superconductivity. Lumsden *et al.* [229] have performed measurements on time-

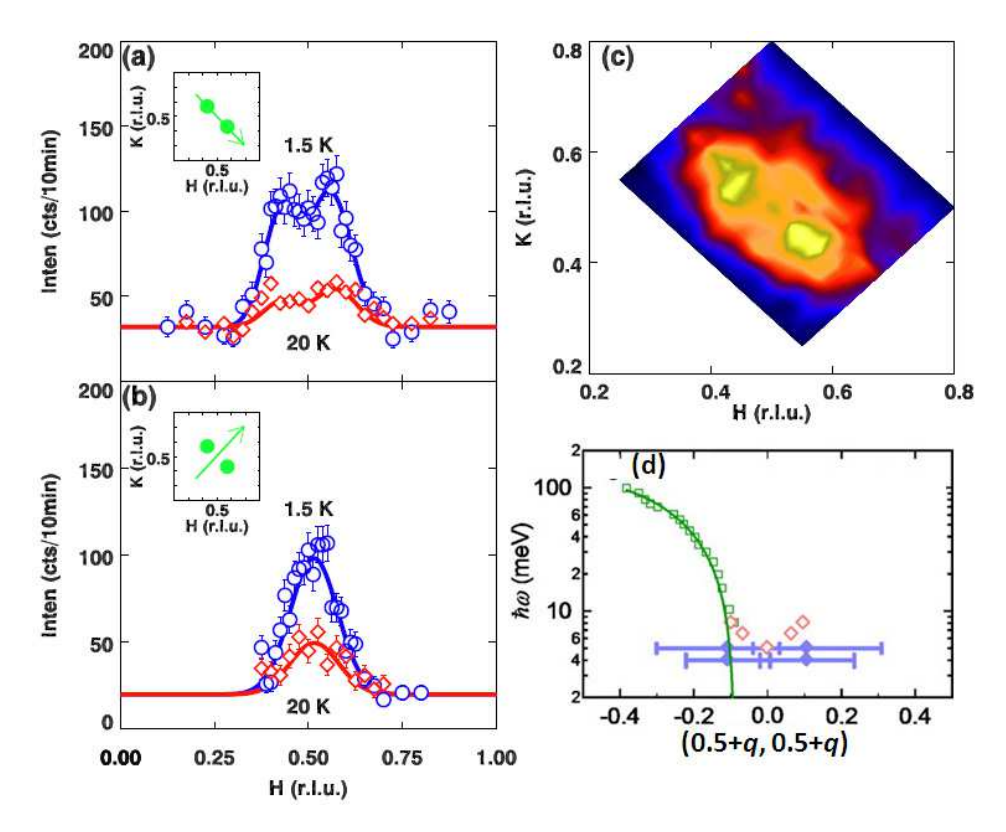


Figure 12. Incommensurate resonance in  $\mathbf{Q}$ , peaking at  $(0.5 \pm \delta, 0.5 \mp \delta)$ , transversely to (0.5, 0.5), at  $\hbar\omega = 6.5$  meV. (a) and (b) show the  $\mathbf{Q}$  scans at 1.5 and 20 K, below and above  $T_c$ , with scans directions shown in the left insets. Upper right inset is obtained by subtracting 20-K data from 1.5-K data. (c) is the plot of the  $\mathbf{Q}$  dependence of the intensity at 6.5 meV at 1.5 K. (d) shows the dispersion from (0.5, 0.5) in semi-log scale. (a)-(c) reprinted from [120]. (d) reprinted from [105]; © 2010 American Physical Society.

of-flight spectrometers which cover a large momentum-energy space on two samples, a non-superconducting  $Fe_{1.04}Te_{0.73}Se_{0.27}$ , and a superconducting  $Fe_{0.51}Se_{0.49}$ . It is clearly shown in figure 13(a) that at 5-7 meV, for the non-superconducting sample, the spectral weight is mostly concentrated around (0.5,0), where static magnetic order is observed. For the superconducting sample, magnetic excitations with a spin resonance near (0.5,0.5) are dominant, as shown in figure 13(b). On the other hand, the high-energy (> 120 meV) spectrum looks qualitatively similar for these two samples [229]. In the non-superconducting parent compound,  $Fe_{1.05}Te$ , spin waves dispersing up to  $\sim 250$  meV have been measured by Lipscombe  $et\,al.$  [238]. These have been modelled in terms of spin waves calculated from a Heisenberg Hamiltonian with nearest- and next-nearest-neighbour couplings [238]; however, a recent study of  $Fe_{1.1}Te$ , identifying distinct patterns of diffuse scattering and anomalous thermal enhancement of the effective moment, raises questions about such an approach [214].

As mentioned previously, the properties of  $Fe_{1+y}Te_{1-x}Se_x$  are sensitive not only to the Se concentration, but also to the amount of excess Fe. Xu *et al.* [106] demonstrated

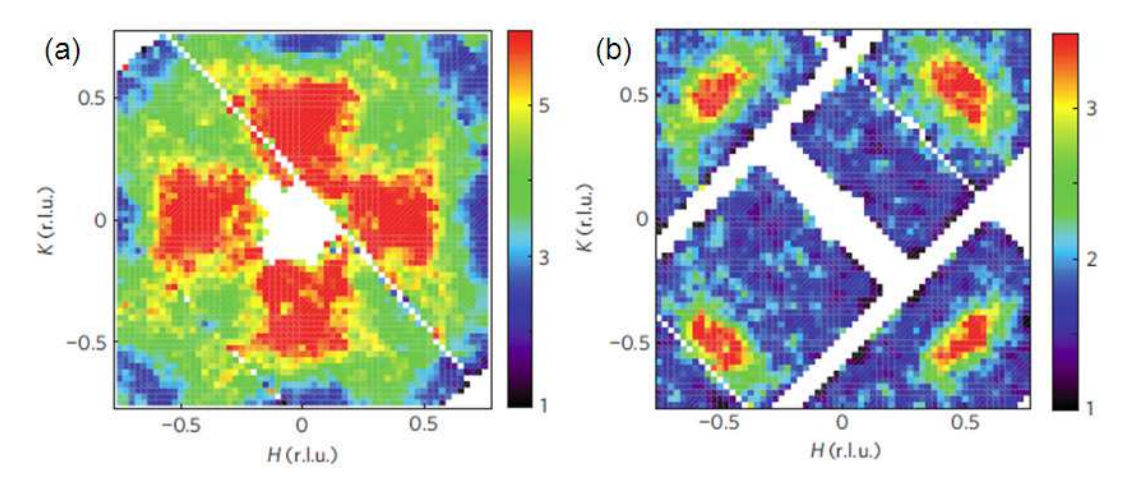


Figure 13. (a) Constant-energy cut of the magnetic excitation spectrum at an energy transfer of  $6 \pm 1$  meV for the non-superconducting sample  $Fe_{1.04}Te_{0.73}Se_{0.27}$  at 5 K. (b) Plot for the superconducting sample  $FeTe_{0.51}Se_{0.49}$  at 3.5 K. Reprinted from [229]. © 2010 Macmillan Publishers Ltd.

this by measuring the magnetic spectrum around (0.5,0) and (0.5,0.5) in four samples: FeTe<sub>0.7</sub>Se<sub>0.3</sub>, Fe<sub>1.05</sub>Te<sub>0.7</sub>Se<sub>0.3</sub>; FeTe<sub>0.5</sub>Se<sub>0.5</sub>, and Fe<sub>1.05</sub>Te<sub>0.55</sub>Se<sub>0.45</sub>. Both samples with y = 0 are superconducting with the same  $T_c$  of 14 K; a resonance in the spin excitation spectrum is observed below  $T_c$  near (0.5,0.5), although the one with x = 0.3 has a smaller superconducting volume fraction, and less spectral weight around (0.5,0.5). Also, there is short-range static magnetic order near (0.5,0) in FeTe<sub>0.7</sub>Se<sub>0.3</sub>, while the sample with x = 0.5 does not exhibit magnetic order, short- or long-ranged, and the low-energy excitations close to (0.5,0) also disappear. With 0.05 extra Fe, superconductivity in both samples is fully suppressed, leading to the absence of the resonance, and the spectral-weight transfers from (0.5,0.5) to (0.5,0). In both samples, there is short-range static order and strong spectral weight around (0.5,0). Recently, Stock *et al.* [239] have shown that by changing y in Fe<sub>1+y</sub>Te, the low-energy magnetic excitation spectrum can be dramatically modified, thus demonstrating the important role of the excess Fe.

## 4.3. Summary

In the parent compound of the 11 system, there is long-range antiferromagnetic order with an ordering temperature of 65 K, and an in-plane wave vector (0.5,0); importantly, no Fermi-surface nesting is found along this wave vector. The direction of the wave vector is different from that of the iron pnicitides by 45°. The magnetic ordering wave vector can become incommensurate with larger amounts of excess Fe.

Upon Se doping, the antiferromagnetic order is suppressed and becomes short-ranged, followed by the appearance of superconductivity. For samples with  $x \approx 0.5$  and robust superconductivity, there is no static order, and the low-energy spin excitations around (0.5,0) also disappear. The spectral weight is shifted to (0.5,0.5), where an incommensurate spin resonance is observed; the spin resonance is demonstrated to be

intimately tied to the superconductivity from both the temperature and magnetic-field dependence. The magnetic excitation spectrum around (0.5, 0.5) shows an interesting anisotropy, which apparently cannot be explained by either a Fermi-surface-nesting or a local-moment model. In Fe<sub>1+y</sub>Se, there is no static order, while there are spin fluctuations which are enhanced near  $T_c$ . The superconducting and magnetic properties of the system can also be modified by adjusting the amount of excess Fe with fixed Se content. The extra Fe is found to enhance the magnetic correlations around (0.5, 0.5).

The results on the evolution of the magnetic excitation spectrum with the tuning parameters (Se/Fe), clearly indicate that static bicollinear magnetic order in the 11 system competes with superconductivity. It appears that only when the system evolves towards fluctuating collinear magnetic correlations, does superconductivity appear; this seems to be universal across all known iron-based superconductor families. Despite these agreements, the origin of the magnetism in the 11 compound is quite controversial. Some believe that the magnetism arises from itinerant electrons [82, 226]. Recently there has been work suggesting a large local moment associated with the low-energy magnetic excitations in a superconducting FeTe<sub>0.35</sub>Se<sub>0.65</sub> sample; this observation is incompatible with predictions from a weakly coupled itinerant picture [240]. The fact that a simple Fermi-surface-nesting picture [204] cannot explain many of the experimental observations [105, 124, 205, 240] leads to arguments for a significant local-moment character to the magnetism [41, 205, 208–213].

For the  $A_x$ Fe<sub>2-y</sub>Se<sub>2</sub> system, it is found that superconductivity is in close proximity to an insulating phase. This feature is different from that in other iron-based superconductors, but mirrors that in the high- $T_c$  cuprates. The coexistence of strong antiferromagnetic order with high  $T_c$  superconductivity is quite unusual, and require further studies to understand whether or not the superconducting pairing mechanism in this system is the same as that in other high- $T_c$  superconductors.

## 5. Conclusions

Thanks to the sustained efforts on sample synthesis for the  $\text{Fe}_{1+y}\text{Te}_{1-x}\text{Se}_x$  system, a large number of high-quality samples have been made available. In particular, by using the Bridgman technique, many large-size, high-quality single crystals have been grown. Measurements performed on these samples yield a plethora of fascinating results. It has been found that the static antiferromagnetic order in the parent compound is centered around the wave vector (0.5,0) with a bicollinear spin structure that competes with superconductivity, while superconducting samples are characterized by a collinear magnetic correlations with magnetic excitations centered around the wave vector (0.5,0.5). The argument that there is an intimate relationship between the spin excitations around (0.5,0.5) and the superconductivity has been reinforced by the temperature and magnetic-field dependence of the resonance. Generally, this system shows strong similarities to other high- $T_c$  superconductors, where it is believed that

spin excitations play a progenitive role in the superconductivity.

For the newly discovered  $A_x$ Fe<sub>2-y</sub>Se<sub>2</sub> superconductors, which have superconducting transition temperatures,  $T_c$ , up to 33 K, crystals can be obtained using the Bridgman technique. This system is unique: i) It has a very different Fermi-surface topology with two electron pockets at the Brillouin zone center; ii) The superconducting phase borders an insulating parent phase, as in the case of the cuprates, but different from all previously investigated iron-based superconductors.

While  $A_x \operatorname{Fe}_{2-y} \operatorname{Se}_2$  has attracted significant attention, there are still many basic questions to be answered. For instance, no report on the spin dynamics in this system has been available so far. This will provide important clues on whether or not this system shares the same basic physics underlying the superconductivity as other high-temperature superconductors. Also, further efforts on obtaining single crystals with improved sample quality and larger size will certainly be needed in order to elucidate many unresolved issues. For the 11 system, sample inhomogeneity remains an issue. Future work to control the stoichiometry more precisely will be helpful.

## 6. Acknowledgements

The work at Brookhaven National Laboratory (J.W., G.X., G.G., and J.M.T.) was supported by the Office of Basic Energy Sciences, Division of Materials Science and Engineering, U.S. Department of Energy, under Contract No. DE-AC02-98CH10886. J.M.T. is also supported in part by the Center for Emergent Superconductivity, an Energy Frontier Research Center. Work at Lawrence Berkeley National Laboratory (J.W. and R.J.B.) was supported by the same Office under Contract No. DE-AC02-05CH11231. The authors thank all of their collaborators listed in the references. We are also grateful to our colleagues and collaborators for allowing us to reproduce their work here.

## References

- [1] H. K. Onnes. The resistance of pure mercury at helium temperatures. *Comm. Leiden.*, 120b, 1911.
- [2] J. Bardeen, L. N. Cooper, and J. R. Schrieffer. Theory of Superconductivity. Phys. Rev., 108:1175, 1957.
- [3] J. G. Bednorz and K. A. Müller. Possible High  $T_c$  Superconductivity in the Ba-La-Cu-O system. Z. Phys. B, 64:189, 1986.
- [4] M. K. Wu, J. R. Ashburn, C. J. Torng, P. H. Hor, R. L. Meng, L. Gao, Z. J. Huang, Y. Q. Wang, and C. W. Chu. Superconductivity at 93 K in a new mixed-phase Y-Ba-Cu-O compound system at ambient pressure. *Phys. Rev. Lett.*, 58:908, 1987.
- [5] Patrick A. Lee, Naoto Nagaosa, and Xiao-Gang Wen. Doping a Mott insulator: Physics of high-temperature superconductivity. *Rev. Mod. Phys.*, 78:17, 2006.

[6] E. W. Carlson, V. J. Emery, S. A. Kivelson, and D. Orgad. The Physics of Conventional and Unconventional Superconductors, chapter Concepts in High Temperature Superconductivity. Springer-Verlag, 2002.

- [7] R. J. Birgeneau, C. Stock, J. M. Tranquada, and K. Yamada. Magnetic neutron scattering in hole doped cuprate superconductors. J. Phys. Soc. Jpn., 75:111003, 2006.
- [8] M. A. Kastner, R. J. Birgeneau, G. Shirane, and Y. Endoh. Magnetic, transport, and optical properties of monolayer copper oxides. Rev. Mod. Phys., 70:897, 1998.
- [9] J. Orenstein and A. J. Millis. Advances in the Physics of High-Temperature Superconductivity. *Science*, 288:468, 2000.
- [10] Yoichi Kamihara, Takumi Watanabe, Masahiro Hirano, and Hideo Hosono. Iron-Based Layered Superconductor  $\text{La}[O_{1-x}F_x]\text{FeAs}$  (x=0.05-0.12) with  $T_c$ =26 K. J. Am. Chem. Soc., 130:3296, 2008.
- [11] Yoichi Kamihara, Hidenori Hiramatsu, Masahiro Hirano, Ryuto Kawamura, Hiroshi Yanagi, Toshio Kamiya, and Hideo Hosono. Iron-Based Layered Superconductor: LaOFeP. J. Am. Chem. Soc., 128:10012, 2006.
- [12] X. H. Chen, T. Wu, G. Wu, R. H. Liu, H. Chen, and D. F. Fang. Superconductivity at 43 K in Samarium-arsenide Oxides SmFeAsO<sub>1-x</sub>F<sub>x</sub>. *Nature*, 453:761, 2008.
- [13] Hiroki Takahashi, Kazumi Igawa, Kazunobu Arii, Yoichi Kamihara, Masahiro Hirano, and Hideo Hosono. Superconductivity at 43 K in an iron-based layered compound LaO<sub>1-x</sub>F<sub>x</sub>FeAs. *Nature*, 453:376, 2008.
- [14] Hijiri Kito, Hiroshi Eisaki, and Akira Iyo. Superconductivity at 54 K in F-Free NdFeAsO<sub>1-y</sub>. J. Phys. Soc. Jpn., 77:063707, 2008.
- [15] Zhi-An Ren, Jie Yang, Wei Lu, Wei Yi, Xiao-Li Shen, Zheng-Cai Li, Guang-Can Che, Xiao-Li Dong, Li-Ling Sun, Fang Zhou, and Zhong-Xian Zhao. Superconductivity in the iron-based F-doped layered quaternary compound  $NdO_{1-x}F_xFeAs$ . Europhys. Lett., 82:57002, 2008.
- [16] Zhi-An Ren, Wei Lu, Jie Yang, Wei Yi, Xiao-Li Shen, Zheng-Cai Li, Guang-Can Che, Xiao-Li Dong, Li-Ling Sun, Fang Zhou, and Zhong-Xian Zhao. Superconductivity at 55 K in iron-based F-doped layered quaternary compound SmO<sub>1-x</sub>F<sub>x</sub>FeAs. *Chin. Phys. Lett.*, 25:2215, 2008.
- [17] Cao Wang, Linjun Li, Shun Chi, Zengwei Zhu, Zhi Ren, Yuke Li, Yuetao Wang, Xiao Lin, Yongkang Luo, Shuai Jiang, Xiangfan Xu, Guanghan Cao, and Zhu'an Xu. Thorium-doping-induced superconductivity up to 56 K in Gd<sub>1-x</sub>Th<sub>x</sub>FeAsO. Europhys. Lett., 83:67006, 2008.
- [18] Athena S. Sefat, Rongying Jin, Michael A. McGuire, Brian C. Sales, David J. Singh, and David Mandrus. Superconductivity at 22 K in Co-Doped BaFe<sub>2</sub>As<sub>2</sub> Crystals. *Phys. Rev. Lett.*, 101:117004, 2008.
- [19] Marianne Rotter, Marcus Tegel, and Dirk Johrendt. Superconductivity at 38 K in the iron arsenide  $Ba_{1-x}K_xFe_2As_2$ . Phys. Rev. Lett., 101:107006, 2008.

[20] G. F. Chen, Z. Li, G. Li, W. Z. Hu, J. Dong, X. D. Zhang, P. Zheng, N. L. Wang, and J. L. Luo. Superconductivity in hole-doped  $(Sr_{1-x}K_x)Fe_2As_2$ . *Chin. Phys. Lett.*, 25:3403, 2008.

- [21] D. S. Inosov, A. Leineweber, Xiaoping Yang, J. T. Park, N. B. Christensen, R. Dinnebier, G. L. Sun, Ch. Niedermayer, D. Haug, P. W. Stephens, J. Stahn, O. Khvostikova, C. T. Lin, O. K. Andersen, B. Keimer, and V. Hinkov. Suppression of the structural phase transition and lattice softening in slightly underdoped Ba<sub>1-x</sub>K<sub>x</sub>Fe<sub>2</sub>As<sub>2</sub> with electronic phase separation. *Phys. Rev. B*, 79:224503, 2009.
- [22] Z. Deng, X. C. Wang, Q.Q. Liu, S. J. Zhang, Y. X. Lv, J. L. Zhu, R.C. Yu, and C.Q. Jin. A new 111 type iron pnictide superconductor LiFeP. *Europhys. Lett.*, 87:3704, 2009.
- [23] X. C. Wang, Q. Q. Liu, Y. X. Lv, W. B. Gao, L. X. Yang, R. C. Yu, F. Y. Li, and C. Q. Jin. The superconductivity at 18 K in LiFeAs system. *Solid State Commun.*, 148:538, 2008.
- [24] M. J. Pitcher, D. R. Parker, P. Adamson, S. J. C. Herkelrath, A. T. Boothroyd, and S. J. Clarke. Structure and superconductivity of LiFeAs. *Chem. Commun.*, 45:5918, 2008.
- [25] C. W. Chu, F. Chen, M. Gooch, A. M. Guloy, B. Lorenz, B. Lv, K. Sasmal, Z. J. Tang, J. H. Tapp, and Y. Y. Xue. The synthesis and characterization of LiFeAs and NaFeAs. *Physica C*, 469:326, 2009.
- [26] Joshua H. Tapp, Zhongjia Tang, Bing Lv, Kalyan Sasmal, Bernd Lorenz, Paul C. W. Chu, and Arnold M. Guloy. LiFeAs: An intrinsic FeAs-based superconductor with  $T_c=18$  K. Phys. Rev. B, 78:060505, 2008.
- [27] Z. Deng, X. C. Wang, Q. Q. Liu, S. J. Zhang, Y. X. Lv, J. L. Zhu, R. C. Yu, and C. Q. Jin. A new "111" type iron pnictide superconductor LiFeP. *Europhys. Lett.*, 87:37004, 2009.
- [28] S. J. Zhang, X. C. Wang, Q. Q. Liu, Y. X. Lv, X. H. Yu, Z. J. Lin, Y. S. Zhao, L. Wang, Y. Ding, H. K. Mao, and C. Q. Jin. Superconductivity at 31 K in the "111"-type iron arsenide superconductor Na<sub>1-x</sub>FeAs induced by pressure. Europhys. Lett., 88:47008, 2009.
- [29] Fong-Chi Hsu, Jiu-Yong Luo, Kuo-Wei Yeh, Ta-Kun Chen, Tzu-Wen Huang, Phillip M. Wu, Yong-Chi Lee, Yi-Lin Huang, Yan-Yi Chu, Der-Chung Yan, and Maw-Kuen Wu. Superconductivity in the PbO-type Structure alpha-FeSe. Proc. Natl. Acad. Sci. USA, 105:14262, 2008.
- [30] Kuo-Wei Yeh, Tzu-Wen Huang, Yi-Lin Huang, Ta-Kun Chen, Fong-Chi Hsu, Phillip M. Wu, Yong-Chi Lee, Yan-Yi Chu, Chi-Liang Chen, Jiu-Yong Luo, Der-Chung Yan, and Maw kuen Wu. Tellurium substitution effect on superconductivity of the  $\alpha$ -phase Iron Selenide. *Europhys. Lett.*, 84:37002, 2008.

[31] B. C. Sales, A. S. Sefat, M. A. McGuire, R. Y. Jin, D. Mandrus, and Y. Mozharivskyj. Bulk superconductivity at 14 K in single crystals of  $Fe_{1+y}Te_xSe_{1-x}$ . *Phys. Rev. B*, 79:094521, 2009.

- [32] G. F. Chen, Z. G. Chen, J. Dong, W. Z. Hu, G. Li, X. D. Zhang, P. Zheng, J. L. Luo, and N. L. Wang. Electronic properties of single-crystalline Fe<sub>1.05</sub>Te and Fe<sub>1.03</sub>Se<sub>0.30</sub>Te<sub>0.70</sub>. Phys. Rev. B, 79:140509(R), 2009.
- [33] M. H. Fang, H. M. Pham, B. Qian, T. J. Liu, E. K. Vehstedt, Y. Liu, L. Spinu, and Z. Q. Mao. Superconductivity close to magnetic instability in Fe(Se<sub>1-x</sub>Te<sub>x</sub>)<sub>0.82</sub>. Phys. Rev. B, 78:224503, 2008.
- [34] Jun Zhao, Q. Huang, Clarina de la Cruz, J. W. Lynn, M. D. Lumsden, Z. A. Ren, Jie Yang, Xiaolin Shen, Xiaoli Dong, Zhongxian Zhao, and Pengcheng Dai. Lattice and magnetic structures of PrFeAsO, PrFeAsO<sub>0.85</sub>F<sub>0.15</sub>, and PrFeAsO<sub>0.85</sub>. Phys. Rev. B, 78:132504, 2008.
- [35] C. Lester, Jiun-Haw Chu, J. G. Analytis, S. C. Capelli, A. S. Erickson, C. L. Condron, M. F. Toney, I. R. Fisher, and S. M. Hayden. Neutron scattering study of the interplay between structure and magnetism in  $Ba(Fe_{1-x}Co_x)_2As_2$ . *Phys. Rev. B*, 79:144523, 2009.
- [36] Y. Qiu, Wei Bao, Q. Huang, T. Yildirim, J. M. Simmons, M. A. Green, J. W. Lynn, Y. C. Gasparovic, J. Li, T. Wu, G. Wu, and X. H. Chen. Crystal Structure and Antiferromagnetic Order in NdFeAsO<sub>1-x</sub>F<sub>x</sub> (x = 0.0 and 0.2) Superconducting Compounds from Neutron Diffraction Measurements. *Phys. Rev. Lett.*, 101:257002, 2008.
- [37] Neeraj Kumar, Songxue Chi, Ying Chen, Kumari Gaurav Rana, A. K. Nigam, A. Thamizhavel, William Ratcliff, II, S. K. Dhar, and Jeffrey W. Lynn. Evolution of the bulk properties, structure, magnetic order, and superconductivity with Ni doping in CaFe<sub>2-x</sub>Ni<sub>x</sub>As<sub>2</sub>. *Phys. Rev. B*, 80:144524, 2009.
- [38] C. de la Cruz, Q. Huang, J. W. Lynn, J. Li, W. Ratcliff, J. L. Zarestzky, H. A. Mook, G. F. Chen, J. L. Luo, N. L. Wang, and P. Dai. Magnetic order close to superconductivity in the iron-based layered LaO<sub>1-x</sub>F<sub>x</sub>FeAs systems. *Nature*, 453:899, 2008.
- [39] Q. Huang, Y. Qiu, Wei Bao, M. A. Green, J. W. Lynn, Y. C. Gasparovic, T. Wu, G. Wu, and X. H. Chen. Neutron-Diffraction Measurements of Magnetic Order and a Structural Transition in the Parent BaFe<sub>2</sub>As<sub>2</sub> Compound of FeAs-Based High-Temperature Superconductors. *Phys. Rev. Lett.*, 101:257003, 2008.
- [40] Ying Chen, J. W. Lynn, J. Li, G. Li, G. F. Chen, J. L. Luo, N. L. Wang, Pengcheng Dai, C. de la Cruz, and H. A. Mook. Magnetic order of the iron spins in NdFeAsO. Phys. Rev. B, 78:064515, 2008.
- [41] M. D. Johannes and I. I. Mazin. Microscopic origin of magnetism and magnetic interactions in ferropnictides. *Phys. Rev. B*, 79:220510(R), 2009.

[42] Stephen D. Wilson, Z. Yamani, C. R. Rotundu, B. Freelon, E. Bourret-Courchesne, and R. J. Birgeneau. Neutron diffraction study of the magnetic and structural phase transitions in BaFe<sub>2</sub>As<sub>2</sub>. *Phys. Rev. B*, 79:184519, 2009.

- [43] M. Kofu, Y. Qiu, Wei bao, S. H. Lee, S. Chang, T. Wu, G. Wu, and X. H. Chen. Neutron scattering investigation of the magnetic order in single crystalline BaFe<sub>2</sub>As<sub>2</sub>. New J. Phys., 11:055001, 2009.
- [44] Jun Zhao, Q. Huang, C. de la Cruz, Shiliang Li, J. W. Lynn, Y. Chen, M. A. Green, G. F. Chen, G. Li, Z. Li, J. L. Luo, N. L. WANG, , and Pengcheng Dai. Structural and magnetic phase diagram of CeFeAsO<sub>1-x</sub>F<sub>x</sub> and its relation to high-temperature superconductivity. *Nature Mater.*, 7:953, 2008.
- [45] H. Luetkens, H. H. Klauss, M. Kraken, F. J. Litterst, T. Dellmann, R. Klingeler, C. Hess, R. Khasanov, A. Amato, C. Baines, J. Hamann-Borrero, N. Leps, A. Kondrat, G. Behr, J. Werner, and B. Buechner. The electronic phase diagram of the LaO<sub>1-x</sub>F<sub>x</sub>FeAs superconductor. *Nature Mater.*, 8:305, 2009.
- [46] A. J. Drew, Ch Niedermayer, P. J. Baker, F. L. Pratt, S. J. Blundell, T. Lancaster, R. H. Liu, G. Wu, X. H. Chen, I. Watanabe, V. K. Malik, A. Dubroka, M. Roessle, K. W. Kim, C. Baines, and C. Bernhard. Coexistence of static magnetism and superconductivity in SmFeAsO<sub>1-x</sub>F<sub>x</sub> as revealed by muon spin rotation. *Nature Mater.*, 8:310, 2009.
- [47] Marianne Rotter, Michael Pangerl, Marcus Tegel, and Dirk Johrendt. Superconductivity and Crystal Structures of  $(Ba_{1-x}K_x)Fe_2As_2$  (x = 0 1). Angew. Chem. Int.. Ed., 47:7949, 2008.
- [48] H. Chen, Y. Ren, Y. Qiu, Wei bao, R. H. Liu, G. Wu, T. Wu, Y. L. Xie, X. F. Wang, Q. Huang, and X. H. Chen. Coexistence of the spin-density-wave and superconductivity in the (Ba,K)Fe<sub>2</sub>As<sub>2</sub>. *Europhys. Lett.*, 85:17006, 2009.
- [49] Lei Fang, Huiqian Luo, Peng Cheng, Zhaosheng Wang, Ying Jia, Gang Mu, Bing Shen, I. I. Mazin, Lei Shan, Cong Ren, and Hai-Hu Wen. Roles of multiband effects and electron-hole asymmetry in the superconductivity and normal-state properties of Ba(Fe<sub>1-x</sub>Co<sub>x</sub>)<sub>2</sub>As<sub>2</sub>. *Phys. Rev. B*, 80:140508(R), 2009.
- [50] Jiun-Haw Chu, James G. Analytis, Chris Kucharczyk, and Ian R. Fisher. Determination of the phase diagram of the electron-doped superconductor  $Ba(Fe_{1-x}Co_x)_2As_2$ . *Phys. Rev. B*, 79:014506, 2009.
- [51] R. Khasanov, M. Bendele, A. Amato, P. Babkevich, A. T. Boothroyd, A. Cervellino, K. Conder, S. N. Gvasaliya, H. Keller, H.-H. Klauss, H. Luetkens, V. Pomjakushin, E. Pomjakushina, and B. Roessli. Coexistence of incommensurate magnetism and superconductivity in  $\text{Fe}_{1+y}\text{Se}_x\text{Te}_{1-x}$ . Phys. Rev. B, 80:140511, 2009.
- [52] T. J. Liu, J. Hu, B. Qian, D. Fobes, Z. Q. Mao, W. Bao, M. Reehuis, S. A. J. Kimber, K. Prokes, S. Matas, D. N. Argyriou, A. Hiess, A. Rotaru, H. Pham, L. Spinu, Y. Qiu, V. Thampy, A. T. Savici, J. A. Rodriguez, and C. Broholm.

From  $(\pi, 0)$  magnetic order to superconductivity with  $(\pi, \pi)$  magnetic resonance in Fe<sub>1.02</sub>(Te<sub>1-x</sub>Se<sub>x</sub>). Nature Mater., 9:716, 2010.

- [53] P. L. Paulose, C. S. Yadav, and K. M. Subhedar. Magnetic phase diagram of  $Fe_{1.1}Te_{1-x}Se_x$ : A comparative study with the stoichiometric superconducting  $FeTe_{1-x}Se_x$  system. *Europhys. Lett.*, 90:27011, 2010.
- [54] N. Katayama, S. Ji, D. Louca, S.-H. Lee, M. Fujita, T. J. Sato, J. S. Wen, Z. J. Xu, G. D. Gu, G. Xu, Z. W. Lin, M. Enoki, S. Chang, K. Yamada, and J. M. Tranquada. Investigation of the spin-glass regime between the antiferromagnetic and superconducting phases in Fe<sub>1+y</sub>Se<sub>x</sub>Te<sub>1-x</sub>. J. Phys. Soc. Jpn., 79:113702, 2010.
- [55] Yoshikazu Mizuguchi and Yoshihiko Takano. Review of Fe Chalcogenides as the Simplest Fe-Based Superconductor. J. Phys. Soc. Jpn., 79:102001, 2010.
- [56] C. Dong, H. Wang, Z. Li, J. Chen, H. Q. Yuan, and M. Fang. Revised Phase Diagram for FeTe1-xSex system with less excess Fe atoms. arXiv:1012.5188, 2010.
- [57] Q. Huang, Jun Zhao, J. W. Lynn, G. F. Chen, J. L. Luo, N. L. Wang, and Pengcheng Dai. Doping evolution of antiferromagnetic order and structural distortion in LaFeAsO<sub>1-x</sub>F<sub>x</sub>. *Phys. Rev. B*, 78:054529, 2008.
- [58] Michael A. McGuire, Andrew D. Christianson, Athena S. Sefat, Brian C. Sales, Mark D. Lumsden, Rongying Jin, E. Andrew Payzant, David Mandrus, Yanbing Luan, Veerle Keppens, Vijayalaksmi Varadarajan, Joseph W. Brill, Raphaël P. Hermann, Moulay T. Sougrati, Fernande Grandjean, and Gary J. Long. Phase transitions in LaFeAsO: Structural, magnetic, elastic, and transport properties, heat capacity and Mössbauer spectra. Phys. Rev. B, 78:094517, 2008.
- [59] I. I. Mazin, D. J. Singh, M. D. Johannes, and M. H. Du. Unconventional Superconductivity with a Sign Reversal in the Order Parameter of LaFeAsO<sub>1-x</sub>F<sub>x</sub>. *Phys. Rev. Lett.*, 101:057003, 2008.
- [60] Kazuhiko Kuroki, Seiichiro Onari, Ryotaro Arita, Hidetomo Usui, Yukio Tanaka, Hiroshi Kontani, and Hideo Aoki. Unconventional Pairing Originating from the Disconnected Fermi Surfaces of Superconducting LaFeAsO<sub>1-x</sub>F<sub>x</sub>. Phys. Rev. Lett., 101:087004, 2008.
- [61] Fengjie Ma and Zhong-Yi Lu. Iron-based layered compound LaFeAsO is an antiferromagnetic semimetal. *Phys. Rev. B*, 78:033111, 2008.
- [62] J. Dong, H. J. Zhang, G. Xu, Z. Li, G. Li, W. Z. Hu, D. Wu, G. F. Chen, X. Dai, J. L. Luo, Z. Fang, and N. L. Wang. Competing Orders and Spin-Density-Wave Instability in  $La(O_{1-x}F_x)$ FeAs. *Europhys. Lett.*, 83:27006, 2008.
- [63] V. Cvetkovic and Z. Tesanovic. Multiband magnetism and superconductivity in Fe-based compounds. *Europhys. Lett.*, 85:37002, 2009.
- [64] S Graser, T A Maier, P J Hirschfeld, and D J Scalapino. Near-degeneracy of several pairing channels in multiorbital models for the Fe pnictides. New J. Phys., 11:025016, 2009.

[65] Hisashi Kotegawa, Satoru Masaki, Yoshiki Awai, Hideki Tou, Yoshikazu Mizuguchi, and Yoshihiko Takano. Evidence for Unconventional Superconductivity in Arsenic-Free Iron-Based Superconductor FeSe: A <sup>77</sup>Se-NMR Study. J. Phys. Soc. Jpn., 77:113703, 2008.

- [66] C. Fang, H. Yao, W. F. Tsai, J. P. Hu, and S. A. Kivelson. Theory of electron nematic order in LaOFeAs. Phys. Rev. B, 77:224509, 2008.
- [67] K Haule and G Kotliar. Coherence–incoherence crossover in the normal state of iron oxypnictides and importance of Hund's rule coupling. New J. Phys., 11:025021, 2009.
- [68] Qimiao Si, Elihu Abrahams, Jianhui Dai, and Jian-Xin Zhu. Correlation effects in the iron pnictides. New J. Phys., 11:045001, 2009.
- [69] I. I. Mazin and M. D. Johannes. A key role for unusual spin dynamics in ferropnictides. *Nature Phys.*, 5:141, 2009.
- [70] Su-Peng Kou, Tao Li, and Zheng-yu Weng. Coexistence of itinerant electrons and local moments in iron-based superconductors. *Europhys. Lett.*, 88:17010, 2009.
- [71] Luca de' Medici, Syed R. Hassan, and Massimo Capone. Genesis of coexisting itinerant and localized electrons in Iron Pnictides. *J. Supercond. Nov. Magn.*, 22:535, 2009.
- [72] Wei-Guo Yin, Chi-Cheng Lee, and Wei Ku. Unified Picture for Magnetic Correlations in Iron-Based Superconductors. Phys. Rev. Lett., 105(10):107004, 2010.
- [73] Ryotaro Arita and Hiroaki Ikeda. Is Fermi-Surface Nesting the Origin of Superconductivity in Iron Pnictides?: A Fluctuation-Exchange-Approximation Study. J. Phys. Soc. Jpn., 78(11):113707, 2009.
- [74] Hiroshi Kontani and Seiichiro Onari. Orbital-Fluctuation-Mediated Superconductivity in Iron Pnictides: Analysis of the Five-Orbital Hubbard-Holstein Model. Phys. Rev. Lett., 104:157001, 2010.
- [75] A. D. Christianson, E. A. Goremychkin, R. Osborn, S. Rosenkranz, M. D. Lumsden, C. D. Malliakas, I.S. Todorov, H. Claus, D. Y. Chung, M. G. Kanatzidis, R. I. Bewley, and T. Guidi. Unconventional superconductivity in Ba<sub>0.6</sub>K<sub>0.4</sub>Fe<sub>2</sub>As<sub>2</sub> from inelastic neutron scattering. *Nature*, 456:930, 2008.
- [76] M. D. Lumsden, A. D. Christianson, D. Parshall, M. B. Stone, S. E. Nagler, G. J. MacDougall, H. A. Mook, K. Lokshin, T. Egami, D. L. Abernathy, E. A. Goremychkin, R. Osborn, M. A. McGuire, A. S. Sefat, R. Jin, B. C. Sales, and D. Mandrus. Two-dimensional resonant magnetic excitation in BaFe<sub>1.84</sub>Co<sub>0.16</sub>As<sub>2</sub>. Phys. Rev. Lett., 102:107005, 2009.
- [77] Songxue Chi, Astrid Schneidewind, Jun Zhao, Leland W. Harriger, Linjun Li, Yongkang Luo, Guanghan Cao, Zhu'an Xu, Micheal Loewenhaupt, Jiangping Hu, and Pengcheng Dai. Inelastic Neutron-Scattering Measurements of a Three-

Dimensional Spin Resonance in the FeAs-Based BaFe<sub>1.9</sub>Ni<sub>0.1</sub>As<sub>2</sub> Superconductor. *Phys. Rev. Lett.*, 102:107006, 2009.

- [78] Shiliang Li, Ying Chen, Sung Chang, Jeffrey W. Lynn, Linjun Li, Yongkang Luo, Guanghan Cao, Zhu'an Xu, and Pengcheng Dai. Spin gap and magnetic resonance in superconducting BaFe<sub>1.9</sub>Ni<sub>0.1</sub>As<sub>2</sub>. Phys. Rev. B, 79:174527, 2009.
- [79] D. S. Inosov, J. T. Park, P. Bourges, D. L. Sun, Y. Sidis, A. Schneidewind, K. Hradil, D. Haug, C. T. Lin, B. Keimer, and V. Hinkov. Normal-State Spin Dynamics and Temperature-Dependent Spin Resonance Energy in an Optimally Doped Iron Arsenide Superconductor. *Nature Phys.*, 6:178, 2010.
- [80] Shin-ichi Shamoto, Motoyuki Ishikado, Andrew D. Christianson, Mark D. Lumsden, Shuichi Wakimoto, Katsuaki Kodama, Akira Iyo, and Masatoshi Arai. Inelastic neutron scattering study of the resonance mode in the optimally doped pnictide superconductor LaFeAsO<sub>0.92</sub>F<sub>0.08</sub>. *Phys. Rev. B*, 82:172508, 2010.
- [81] Yiming Qiu, Wei Bao, Y. Zhao, Collin Broholm, V. Stanev, Z. Tesanovic, Y. C. Gasparovic, S. Chang, Jin Hu, Bin Qian, Minghu Fang, and Zhiqiang Mao. Spin Gap and Resonance at the Nesting Wave Vector in Superconducting FeSe<sub>0.4</sub>Te<sub>0.6</sub>. Phys. Rev. Lett., 103:067008, 2009.
- [82] H. A. Mook, M. D. Lumsden, A. D. Christianson, S. E. Nagler, Brian C. Sales, Rongying Jin, Michael A. McGuire, Athena S. Sefat, D. Mandrus, T. Egami, and Clarina dela Cruz. Unusual Relationship between Magnetism and Superconductivity in FeTe<sub>0.5</sub>Se<sub>0.5</sub>. Phys. Rev. Lett., 104:187002, 2010.
- [83] Jinsheng Wen, Guangyong Xu, Zhijun Xu, Zhi Wei Lin, Qiang Li, Ying Chen, Songxue Chi, Genda Gu, and J. M. Tranquada. Effect of magnetic field on the spin resonance in FeTe<sub>0.5</sub>Se<sub>0.5</sub> as seen via inelastic neutron scattering. *Phys. Rev. B*, 81:100513(R), 2010.
- [84] Kenji Ishida, Yusuke Nakai, and Hideo Hosono. To What Extent Iron-Pnictide New Superconductors Have Been Clarified: A Progress Report. J. Phys. Soc. Jpn., 78:062001, 2009.
- [85] Hideo Hosono. Layered Iron Pnictide Superconductors: Discovery and Current Status. J. Phys. Soc. Jpn. Supplement C, 77:1, 2008.
- [86] Jeffrey W. Lynn and Pengcheng Dai. Neutron Studies of the Iron-based Family of High T<sub>C</sub> Magnetic Superconductors. Physcia C, 469:469, 2009.
- [87] M. D. Lumsden and A. D. Christianson. Magnetism in Fe-based superconductors. J. Phys.: Conden. Matter, 22:203203, 2010.
- [88] Hideo Hosono. Two classes of superconductors discovered in our material research: Iron-based high temperature superconductor and electride superconductor. *Physica C*, 469:314, 2009.
- [89] M.K. Wu, F.C. Hsu, K.W. Yeh, T.W. Huang, J.Y. Luo, M.J. Wang, H.H. Chang, T.K. Chen, S.M. Rao, B.H. Mok, C.L. Chen, Y.L. Huang, C.T. Ke, P.M. Wu,

A.M. Chang, C.T. Wu, and T.P. Perng. The development of the superconducting PbO-type  $\beta$ -FeSe and related compounds. *Physica C*, 469:340, 2009.

- [90] Paul C. Canfield and Sergey L. Bud'ko. FeAs-Based Superconductivity: A Case Study of the Effects of Transition Metal Doping on BaFe<sub>2</sub>As<sub>2</sub>. Annual Rev. Conden. Matter Phys., 1:27, 2010.
- [91] D. C. Johnston. The puzzle of high temperature superconductivity in layered iron pnictides and chalcogenides. *Adv. Phys.*, 59:803, 2010.
- [92] I. Mazin. Superconductivity gets an iron boost. Nature, 464:183, 2010.
- [93] Johnpierre Paglione and Richard L. Greene. High-temperature superconductivity in iron-based materials. *Nature Phys.*, 6:645, 2010.
- [94] Jiangang Guo, Shifeng Jin, Gang Wang, Shunchong Wang, Kaixing Zhu, Tingting Zhou, Meng He, and Xiaolong Chen. Superconductivity in the iron selenide  $K_xFe_2Se_2$  ( $0 \le x \le 1.0$ ). Phys. Rev. B, 82:180520, 2010.
- [95] Y. Mizuguchi, H. Takeya, Y. Kawasaki, T. Ozaki, S. Tsuda, T. Yamaguchi, and Y. Takano. Transport properties of the new Fe-based superconductor  $K_x$ Fe<sub>2</sub>Se<sub>2</sub> ( $T_c = 33$  K). Appl. Phys. Lett., 98:042511, 2011.
- [96] A. F. Wang, J. J. Ying, Y. J. Yan, R. H. Liu, X. G. Luo, Z. Y. Li, X. F. Wang, M. Zhang, G. J. Ye, P. Cheng, Z. J. Xiang, and X. H. Chen. Superconductivity at 32 K in single-crystalline Rb<sub>x</sub>Fe<sub>2-y</sub>Se<sub>2</sub>. Phys. Rev. B, 83(6):060512, 2011.
- [97] A Krzton-Maziopa, Z Shermadini, E Pomjakushina, V Pomjakushin, M Bendele, A Amato, R Khasanov, H Luetkens, and K Conder. Synthesis and crystal growth of  $Cs_{0.8}(FeSe_{0.98})_2$ : a new iron-based superconductor with  $T_c=27$  K. J. Physs. Conden. Matter, 23:052203, 2011.
- [98] Hang-Dong Wang, Chi-Heng Dong, Zu-Juan Li, Qian-Hui Mao, Sha-Sha Zhu, Chun-Mu Feng, H. Q. Yuan, and Ming-Hu Fang. Superconductivity at 32 K and anisotropy in Tl<sub>0.58</sub>Rb<sub>0.42</sub>Fe<sub>1.72</sub>Se<sub>2</sub> crystals. *Europhys. Lett.*, 93:47004, 2011.
- [99] Y. Mizuguchi, K. Deguchi, Y. Kawasaki, T. Ozaki, M. Nagao, S. Tsuda, T. Yamaguchi, and Y. Takano. Superconductivity in oxygen-annealed  $\text{FeTe}_{1-x}S_x$  single crystal. *J. Appl. Phys.*, 109:013914, 2011.
- [100] T. J. Liu, X. Ke, B. Qian, J. Hu, D. Fobes, E. K. Vehstedt, H. Pham, J. H. Yang, M. H. Fang, L. Spinu, P. Schiffer, Y. Liu, and Z. Q. Mao. Charge-carrier localization induced by excess Fe in the superconductor  $Fe_{1+y}Te_{1-x}Se_x$ . *Phys. Rev. B*, 80:174509, 2009.
- [101] Takashi Noji, Takumi Suzuki, Haruki Abe, Tadashi Adachi, Masatsune Kato, and Yoji Koike. Growth, Annealing Effects on Superconducting and Magnetic Properties, and Anisotropy of  $\text{FeSe}_{1-x}\text{Te}_x$  (0.5  $\leq x \leq$  1) Single Crystals. *J. Phys. Soc. Jpn.*, 79:084711, 2010.
- [102] Jinhu Yang, Mami Matsui, Masatomo Kawa, Hiroto Ohta, Chishiro Michioka, Chiheng Dong, Hangdong Wang, Huiqiu Yuan, Minghu Fang, and Kazuyoshi

Yoshimura. Magnetic and Superconducting Properties in Single Crystalline  $\text{Fe}_{1+\delta}\text{Te}_{1-x}\text{Se}_x$  (x < 0.50) System. J. Phys. Soc. Jpn., 79:074704, 2010.

- [103] Jinsheng Wen, Guangyong Xu, Zhijun Xu, Zhi Wei Lin, Qiang Li, W. Ratcliff, Genda Gu, and J. M. Tranquada. Short-range incommensurate magnetic order near the superconducting phase boundary in  $\text{Fe}_{1+\delta}\text{Te}_{1-x}\text{Se}_x$ . Phys. Rev. B, 80:104506, 2009.
- [104] C. C. Homes, A. Akrap, J. S. Wen, Z. J. Xu, Z. W. Lin, Q. Li, and G. D. Gu. Electronic correlations and unusual superconducting response in the optical properties of the iron-chalcogenide FeTe<sub>0.55</sub>Se<sub>0.45</sub>. *Phys. Rev. B*, 81:180508(R), 2010.
- [105] S.-H. Lee, Guangyong Xu, W. Ku, J. S. Wen, C. C. Lee, N. Katayama, Z. J. Xu, S. Ji, Z. W. Lin, G. D. Gu, H.-B. Yang, P. D. Johnson, Z.-H. Pan, T. Valla, M. Fujita, T. J. Sato, S. Chang, K. Yamada, and J. M. Tranquada. Coupling of spin and orbital excitations in the iron-based superconductor FeTe<sub>0.5</sub>Se<sub>0.5</sub>. Phys. Rev. B, 81:220502(R), 2010.
- [106] Zhijun Xu, Jinsheng Wen, Guangyong Xu, Qing Jie, Zhiwei Lin, Qiang Li, Songxue Chi, D. K. Singh, Genda Gu, and J. M. Tranquada. Disappearance of static magnetic order and evolution of spin fluctuations in  $\text{Fe}_{1+\delta}\text{Se}_x\text{Te}_{1-x}$ . Phys. Rev. B, 82:104525, 2010.
- [107] I. Pallecchi, G. Lamura, M. Tropeano, M. Putti, R. Viennois, E. Giannini, and D. Van der Marel. Seebeck effect in  $\text{Fe}_{1+x}\text{Te}_{1-y}\text{Se}_y$  single crystals. *Phys. Rev. B*, 80:214511, 2009.
- [108] T. Taen, Y. Tsuchiya, Y. Nakajima, and T. Tamegai. Superconductivity at  $T_c \sim 14$  K in single-crystalline FeTe<sub>0.61</sub>Se<sub>0.39</sub>. *Phys. Rev. B*, 80:092502, 2009.
- [109] Minghu Fang, Jinhu Yang, F. F. Balakirev, Y. Kohama, J. Singleton, B. Qian, Z. Q. Mao, Hangdong Wang, and H. Q. Yuan. Weak anisotropy of the superconducting upper critical field in Fe<sub>1.11</sub>Te<sub>0.6</sub>Se<sub>0.4</sub> single crystals. *Phys. Rev. B*, 81:020509, 2010.
- [110] Rongwei Hu, Emil S. Bozin, J. B. Warren, and C. Petrovic. Superconductivity, magnetism, and stoichiometry of single crystals of  $\text{Fe}_{1+y}(\text{Te}_{1-x}S_x)_z$ . Phys. Rev. B, 80:214514, 2009.
- [111] K. W. Yeh, C. T. Ke, T. W. Huang, T. K. Chen, Y. L. Huang, P. M. Wu, and M. K. Wu. Superconducting  $FeSe_{1-x}Te_x$  Single Crystals Grown by Optical Zone-Melting Technique. Cryst. Growth Des., 9:4847, 2009.
- [112] U. Patel, J. Hua, S. H. Yu, S. Avci, Z. L. Xiao, H. Claus, J. Schlueter, V. V. Vlasko-Vlasov, U. Welp, and W. K. Kwok. Growth and superconductivity of FeSe<sub>x</sub> crystals. *Appl. Phys. Lett.*, 94:082508, 2009.
- [113] S B Zhang, Y P Sun, X D Zhu, X B Zhu, B S Wang, G Li, H C Lei, X Luo, Z R Yang, W H Song, and J M Dai. Crystal growth and superconductivity of FeSe<sub>x</sub>. Supercond. Sci. Technol., 22:015020, 2009.

[114] R. Hu, H. Lei, M. Abeykoon, E. S. Bozin, S. J. L. Billinge, J. B. Warren, T. Siegrist, and C. Petrovic. Synthesis, Magnetism and Crystal Structure in  $\beta$ -Fe<sub>1.00(2)</sub>Se<sub>1.00(3)</sub> Single Crystals. unpublished.

- [115] D. M. Wang, J. B. He, T. Xia, and G. F. Chen. The effect of varying Fe-content on transport properties of K intercalated iron selenide  $K_xFe_{2-y}Se_2$ . arXiv:1101.0789, 2011.
- [116] H. Lei and C. Petrovic. Anisotropy in transport and magnetic properties of  $K_x Fe_{2-y} Se_2$ . arXiv:1102.1010, 2011.
- [117] J. Ying, X. F. Wang, X. G. Luo, A. F. Wang, M. Zhang, Y. J. Yan, Z. J. Xiang, R. H. Liu, P. Cheng, G. J. Ye, and X. H. Chen. Superconductivity and Magnetic Properties of high-quality single crystals of  $A_x$ Fe<sub>2</sub>Se<sub>2</sub> (A = K and Cs). arXiv:1012.5552, 2010.
- [118] M. Fang, H. Wang, C. Dong, Z. Li, C. Feng, J. Chen, and H. Q. Yuan. Febased high temperature superconductivity with  $T_c = 31$  K bordering an insulating antiferromagnet in  $(Tl,K)Fe_xSe_2$  Crystals. arXiv:1012.5236, 2010.
- [119] Z. Gao, Y. Qi, L. Wang, C. Yao, D. Wang, X. Zhang, and Y. Ma. Upper fields and critical current density of K<sub>0.58</sub>Fe<sub>1.56</sub>Se<sub>2</sub> single crystals grown by one step technique. *arXiv:1103.2904*, 2011.
- [120] Jinsheng Wen. Interplay between magnetism and superconductivity in high-temperature superconductors  $La_{2-x}Ba_xCuO_4$  and  $Fe_{1+y}Te_{1-x}Se_x$ : crystal growth and neutron scattering studies. PhD thesis, Stony Brook University, 2010.
- [121] Zhijun Xu, Jinsheng Wen, Guangyong Xu, Sujung Han, Qiang Li, J. M. Tranquada, and Genda Gu. unpublished.
- [122] T. M. McQueen, A. J. Williams, P. W. Stephens, J. Tao, Y. Zhu, V. Ksenofontov, F. Casper, C. Felser, and R. J. Cava. Tetragonal-to-Orthorhombic Structural Phase Transition at 90 K in the Superconductor Fe<sub>1.01</sub>Se. *Phys. Rev. Lett.*, 103:057002, 2009.
- [123] Serena Margadonna, Yasuhiro Takabayashi, Martin T. McDonald, Karolina Kasperkiewicz, Yoshikazu Mizuguchi, Yoshihiko Takano, Andrew N. Fitch, Emmanuelle Suard, and Kosmas Prassides. Crystal structure of the new  $FeSe_{1-x}$  superconductor. *Chem. Commun.*, page 5607, 2008.
- [124] Wei Bao, Y. Qiu, Q. Huang, M. A. Green, P. Zajdel, M. R. Fitzsimmons, M. Zhernenkov, M. Fang, B. Qian, E. K. Vehstedt, J. Yang, H. M. Pham, L. Spinu, and Z. Q. Mao. Tunable  $(\delta \pi, \delta \pi)$ -Type Antiferromagnetic Order in  $\alpha$ -Fe(Te,Se) Superconductors. *Phys. Rev. Lett.*, 102:247001, 2009.
- [125] Shiliang Li, Clarina de la Cruz, Q. Huang, Y. Chen, J. W. Lynn, Jiangping Hu, Yi-Lin Huang, Fong-Chi Hsu, Kuo-Wei Yeh, Maw kuen Wu, and Pengcheng Dai. First-order magnetic and structural phase transitions in  $\text{Fe}_{1+y}\text{Se}_x\text{Te}_{1-x}$ . Phys. Rev. B, 79:054503, 2009.

[126] A. Martinelli, A. Palenzona, M. Tropeano, C. Ferdeghini, M. Putti, M. R. Cimberle, T. D. Nguyen, M. Affronte, and C. Ritter. From antiferromagnetism to superconductivity in  $\text{Fe}_{1+y}\text{Te}_{1-x}\text{Se}_x$  ( $0 \le x \le 0.20$ ): Neutron powder diffraction analysis. *Phys. Rev. B*, 81:094115, 2010.

- [127] Y. Mizuguchi, F. Tomioka, S. Tsuda, T. Yamaguchi, and Y. Takano. Superconductivity in S-substituted FeTe. *Appl. Phys. Lett.*, 94:012503, 2009.
- [128] Y. Mizuguchi, F. Tomioka, S. Tsuda, T. Yamaguchi, and Y. Takano. FeTe as a candidate material for new iron-based superconductor. *Physica C*, 469:1027, 2009.
- [129] A. Martinelli, A. Palenzona, M. Tropeano, C. Ferdeghini, M. Putti, M. R. Cimberle, T. D. Nguyen, M. Affronte, and C. Ritter. From antiferromagnetism to superconductivity in Fe1 + yTe1 xSex ( $\leq x \leq 0.20$ ): Neutron powder diffraction analysis. *Phys. Rev. B*, 81:094115, 2010.
- [130] Yoshikazu Mizuguchi, Fumiaki Tomioka, Shunsuke Tsuda, Takahide Yamaguchi, and Yoshihiko Takano. Substitution Effects on FeSe Superconductor. J. Phys. Soc. Jpn., 78:074712, 2009.
- [131] Weidong Si, Zhi-Wei Lin, Qing Jie, Wei-Guo Yin, Juan Zhou, Genda Gu, P. D. Johnson, and Qiang Li. Enhanced superconducting transition temperature in FeSe<sub>0.5</sub>Te<sub>0.5</sub> thin films. *Appl. Phys. Lett.*, 95:052504, 2009.
- [132] Takanori Kida, Takahiro Matsunaga, Masayuki Hagiwara, Yoshikazu Mizuguchi, Yoshihiko Takano, and Koichi Kindo. Upper critical fields of the 11-system iron-chalcogenide superconductor FeSe<sub>0.25</sub>Te<sub>0.75</sub>. J. Phys. Soc. Jpn., 78:113701, 2009.
- [133] C S Yadav and P L Paulose. Upper critical field, lower critical field and critical current density of FeTe<sub>0.60</sub> Se<sub>0.40</sub> single crystals. New J. Phys., 11:103046, 2009.
- [134] T. M. McQueen, Q. Huang, V. Ksenofontov, C. Felser, Q. Xu, H. Zandbergen, Y. S. Hor, J. Allred, A. J. Williams, D. Qu, J. Checkelsky, N. P. Ong, and R. J. Cava. Extreme sensitivity of superconductivity to stoichiometry in Fe<sub>1+ $\delta$ </sub>Se. *Phys. Rev. B*, 79:014522, 2009.
- [135] S. Rößler, Dona Cherian, S. Harikrishnan, H. L. Bhat, Suja Elizabeth, J. A. Mydosh, L. H. Tjeng, F. Steglich, and S. Wirth. Disorder-driven electronic localization and phase separation in superconducting Fe<sub>1+y</sub>Te<sub>0.5</sub>Se<sub>0.5</sub> single crystals. *Phys. Rev. B*, 82:144523, 2010.
- [136] M. Bendele, P. Babkevich, S. Katrych, S. N. Gvasaliya, E. Pomjakushina, K. Conder, B. Roessli, A. T. Boothroyd, R. Khasanov, and H. Keller. Tuning the superconducting and magnetic properties of Fe<sub>y</sub>Se<sub>0.25</sub>Te<sub>0.75</sub> by varying the iron content. *Phys. Rev. B*, 82:212504, 2010.
- [137] E. E. Rodriguez, C. Stock, P. Hsieh, N. Butch, J. Paglione, and M. A. Green. Interstitial Iron Controlled Superconductivity in  $Fe_{1+x}Te_{0.7}Se_{0.3}$ . arXiv:1012.0590, 2010.
- [138] S. Medvedev, T. M. McQueen, I. Trojan, T. Palasyuk, M. I. Eremets, R. J. Cava, S. Naghavi, F. Casper, V. Ksenofontov, G. Wortmann, and C. Felser. Electronic

and magnetic phase diagram of  $\alpha$ -Fe<sub>1.01</sub>Se with superconductivity at 36.7 K under pressure. *Nature Mater.*, 8:630, 2009.

- [139] S. Margadonna, Y. Takabayashi, Y. Ohishi, Y. Mizuguchi, Y. Takano, T. Kagayama, T. Nakagawa, M. Takata, and K. Prassides. Pressure evolution of the low-temperature crystal structure and bonding of the superconductor FeSe  $(T_c = 37 \text{ K})$ . Phys. Rev. B, 80:064506, 2009.
- [140] Satoru Masaki, Hisashi Kotegawa, Yudai Hara, Hideki Tou, Keizo Murata, Yoshikazu Mizuguchi, and Yoshihiko Takano. Precise Pressure Dependence of the Superconducting Transition Temperature of FeSe: Resistivity and <sup>77</sup>Se-NMR Study. J. Phys. Soc. Jpn., 78:063704, 2009.
- [141] V. G. Tissen, E. G. Ponyatovsky, M. V. Nefedova, A. N. Titov, and V. V. Fedorenko. Effects of pressure-induced phase transitions on superconductivity in single-crystal Fe<sub>1.02</sub>Se. *Phys. Rev. B*, 80:092507, 2009.
- [142] Yoshikazu Mizuguchi, Fumiaki Tomioka, Shunsuke Tsuda, Takahide Yamaguchi, and Yoshihiko Takano. Superconductivity at 27 K in tetragonal FeSe under high pressure. *Appl. Phys. Lett.*, 93:152505, 2008.
- [143] K. Miyoshi, Y. Takaichi, E. Mutou, K. Fujiwara, and J. Takeuchi. Anomalous Pressure Dependence of the Superconducting Transition Temperature in  $FeSe_{1-x}$  Studied by DC Magnetic Measurements. J. Phys. Soc. Jpn, 78:093703, 2009.
- [144] Kazumasa Horigane, Nao Takeshita, Chul-Ho Lee, Haruhiro Hiraka, and Kazuyoshi Yamada. First Investigation of Pressure Effects on Transition from Superconductive to Metallic Phase in FeSe<sub>0.5</sub>Te<sub>0.5</sub>. J. Phys. Soc. Japn., 78:063705, 2009.
- [145] Yoshikazu Mizuguchi, Fumiaki Tomioka, Keita Deguchi, Shunsuke Tsuda, Takahide Yamaguchi, and Yoshihiko Takano. Pressure effects on FeSe family superconductors. *Physica C*, 470:S353, 2010.
- [146] Y Mizuguchi, Y Hara, K Deguchi, S Tsuda, T Yamaguchi, K Takeda, H Kotegawa, H Tou, and Y Takano. Anion height dependence of  $T_c$  for the Fe-based superconductor. Supercond. Sci. Technol., 23:054013, 2010.
- [147] Nathalie C. Gresty, Yasuhiro Takabayashi, Alexey Y. Ganin, Martin T. McDonald, John B. Claridge, Duong Giap, Yoshikazu Mizuguchi, Yoshihiko Takano, Tomoko Kagayama, Yasuo Ohishi, Masaki Takata, Matthew J. Rosseinsky, Serena Margadonna, and Kosmas Prassides. Structural Phase Transitions and Superconductivity in Fe<sub>1+δ</sub>Se<sub>0.57</sub>Te<sub>0.43</sub> at Ambient and Elevated Pressures. J. Am. Chem. Soc., 131:16944, 2009.
- [148] Hironari Okada, Hiroyuki Takahashi, Yoshikazu Mizuguchi, Yoshihiko Takano, and Hiroki Takahashi. Successive Phase Transitions under High Pressure in FeTe<sub>0.92</sub>. J. Phys. Soc. Jpn., 78:083709, 2009.
- [149] Chao Zhang, Wei Yi, Liling Sun, Xiao-Jia Chen, Russell J. Hemley, Hokwang Mao, Wei Lu, Xiaoli Dong, Ligang Bai, Jing Liu, Antonio F. Moreira

Dos Santos, Jamie J. Molaison, Christopher A. Tulk, Genfu Chen, Nanlin Wang, and Zhongxian Zhao. Pressure-induced lattice collapse in the tetragonal phase of single-crystalline  $Fe_{1.05}Te$ . Phys. Rev. B, 80:144519, 2009.

- [150] Y. Han, W. Y. Li, L. X. Cao, X. Y. Wang, B. Xu, B. R. Zhao, Y. Q. Guo, and J. L. Yang. Superconductivity in Iron Telluride Thin Films under Tensile Stress. *Phys. Rev. Lett.*, 104:017003, 2010.
- [151] Evan Lyle Thomas, Winnie Wong-Ng, Daniel Phelan, and Jasmine N. Millican. Thermopower of Co-doped FeSe. J. Appl. Phys., 105:073906, 2009.
- [152] A. J. Williams, T. M. McQueen, V. Ksenofontov, C. Felser, and R. J. Cava. The metal-insulator transition in Fe<sub>1.01-x</sub>Cu<sub>x</sub>Se. J. Phys. Condens. Matter, 21:305701, 2009.
- [153] Tzu-Wen Huang, Ta-Kun Chen, Kuo-Wei Yeh, Chung-Ting Ke, Chi Liang Chen, Yi-Lin Huang, Fong-Chi Hsu, Maw-Kuen Wu, Phillip M. Wu, Maxim Avdeev, and Andrew J. Studer. Doping-driven structural phase transition and loss of superconductivity in  $M_x$ Fe<sub>1-x</sub>Se<sub> $\delta$ </sub> (M = Mn, Cu). Phys. Rev. B, 82:104502, 2010.
- [154] S. B. Zhang, H.C. Lei, X.D. Zhu, G. Li, B.S. Wang, L.J. Li, X.B. Zhu, W.H. Song, Z.R. Yang, and Y.P. Sun. Divergency of SDW and structure transition in  $Fe_{1-x}Ni_xSe_{0.82}$  superconductors. *Physica C*, 469:1958, 2009.
- [155] D. J. Gawryluk, J. Fink-Finowicki, A. Wisniewski, R. Puzniak, V. Domukhovski, R. Diduszko, M. Kozlowski, and M. Berkowski. Growth conditions, structure, and superconductivity of pure and metal-doped  $\text{FeTe}_{1-x}\text{Se}_x$  single crystals. arXiv:1010.4217, 2010.
- [156] R. Shipra, H. Takeya, K. Hirata, and A. Sundaresan. Effects of Ni and Co doping on the physical properties of tetragonal FeSe<sub>0.5</sub>Te<sub>0.5</sub> superconductor. *Physica C*, 470:528, 2010.
- [157] P. Zajdel, M. Zubko, J. Kusz, and M. A. Green. Single crystal growth and structural properties of iron telluride doped with nickel. *Cryst. Res. Technol.*, 45:1316, 2010.
- [158] B. Zeng, B. Shen, G. Chen, J. He, D. Wang, C. Li, and H.-H. Wen. Nodeless superconductivity in  $K_x Fe_{2-y} Se_2$  single crystals revealed by low temperature specific heat. arXiv:1101.5117, 2011.
- [159] R. Hu, K. Cho, H. Kim, H. Hodovanets, W. E. Straszheim, M. A. Tanatar, R. Prozorov, S. L. Bud'ko, and P. C. Canfield. Anisotropic magnetism, resistivity, London penetration depth and magneto-optical imaging of superconducting K<sub>0.86</sub>Fe<sub>1.84</sub>Se<sub>2</sub> single crystals. arXiv:1102.1931, 2011.
- [160] Z. Li, X. Ma, H. Pang, and F. Li. Evidence of spin excitation gap in K<sub>0.86</sub>Fe<sub>1.73</sub>Se<sub>2</sub> superconductor as revealed by Mössbauer spectroscopy. arXiv:1103.0098, 2011.
- [161] D. A. Torchetti, M. Fu, D. C. Christensen, K. J. Nelson, T. Imai, H. C. Lei, and C. Petrovic. <sup>77</sup>Se NMR investigation of the  $K_xFe_{2-y}Se_2$  high- $T_c$  superconductor  $(T_c = 33 \text{ K})$ . Phys. Rev. B, 83:104508, 2011.

[162] R. H. Yuan, T. Dong, G. F. Chen, J. B. He, D. M. Wang, and N. L. Wang. Observation of a small superconducting energy gap in K<sub>0.7</sub>Fe<sub>1.8</sub>Se<sub>2</sub> by optical spectroscopy. *arXiv:1102.1381*, 2011.

- [163] E. D. Mun, M. M. Altarawneh, C. H. Mielke, V. S. Zapf, R. Hu, S. L. Bud'ko, and P. C. Canfield. Anisotropic  $H_{c2}$  of  $K_{0.8}Fe_{1.76}Se_2$  determined up to 60 T. arXiv:1103.0507, 2011.
- [164] H. Kotegawa, Y. Hara, H. Nohara, H. Tou, Y. Mizuguchi, H. Takeya, and Y. Takano. Superconducting Symmetry and Magnetic Correlations in K<sub>0.8</sub>Fe<sub>2</sub>Se<sub>2</sub>: A <sup>77</sup>Se NMR Study. arXiv:1101.4572, 2011.
- [165] V. Y. Pomjakushin, E. V. Pomjakushina, A. Krzton-Maziopa, K. Conder, and Z. Shermadini. Room temperature antiferromagnetic order in superconducting  $X_y$ Fe<sub>2-x</sub>Se<sub>2</sub>, (X = Rb, K): a powder neutron diffraction study. arXiv:1102.3380, 2011.
- [166] X. G. Luo, X. F. Wang, J. J. Ying, Y. J. Yan, Z. Y. Li, M. Zhang, A. F. Wang, P. Cheng, Z. J. Xiang, G. J. Ye, R. H. Liu, and X. H. Chen. Crystal structure, physical properties and superconductivity in  $A_x$ Fe<sub>2</sub>Se<sub>2</sub> single crystals. arXiv:1101.5670, 2011.
- [167] G. Seyfarth, D. Jaccard, P. Pedrazzini, A. Krzton-Maziopa, E. Pomjakushina, K. Conder, and Z. Shermadini. Pressure cycle of superconducting Cs<sub>0.8</sub>Fe<sub>2</sub>Se<sub>2</sub>: a transport study. arXiv:1102.2464, 2011.
- [168] V. Y. Pomjakushin, D. V. Sheptyakov, E. V. Pomjakushina, A. Krzton-Maziopa, K. Conder, D. Chernyshov, V. Svitlyk, and Z. Shermadini. Iron vacancy superstructure and possible room temperature antiferromagnetic order in superconducting  $Cs_yFe_{2-x}Se_2$ . arXiv:1102.1919, 2011.
- [169] R. H. Liu, X. G. Luo, M. Zhang, A. F. Wang, J. J. Ying, X. F. Wang, Y. J. Yan, Z. J. Xiang, P. Cheng, G. J. Ye, Z. Y. Li, and X. H. Chen. Coexistence of superconductivity and antiferromagnetism in single crystals  $A_{0.8}$ Fe<sub>2-y</sub>Se<sub>2</sub> (A = K, Rb, Cs, Tl/K and Tl/Rb): evidence from magnetization and resistivity. arXiv:1102.2783, 2011.
- [170] Z. Shermadini, A. Krzton-Maziopa, M. Bendele, R. Khasanov, H. Luetkens, K. Conder, E. Pomjakushina, S. Weyeneth, V. Pomjakushin, O. Bossen, and A. Amato. Coexistence of Magnetism and Superconductivity in the Iron-based Compound Cs<sub>0.8</sub>(FeSe<sub>0.98</sub>)<sub>2</sub>. arXiv:1101.1873, 2011.
- [171] H. Lei, K. Wang, J. B. Warren, and C. Petrovic. Magnetic and superconducting phase diagram of  $K_xFe_{2-y}Se_{2-z}S_z$  (0  $\leq z \leq$  2). arXiv:1102.2434, 2011.
- [172] L. Li, Z. R. Yang, Z. T. Zhang, W. Tong, C. J. Zhang, S. Tan, and Y. H. Zhang. Coexistence of superconductivity and magnetism in K<sub>0.8</sub>Fe<sub>2</sub>Se<sub>1.4</sub>S<sub>0.4</sub>. arXiv:1101.5327, 2011.
- [173] T. Zhou, X. Chen, J. Guo, G. Wang, X. Lai, S. Wang, S. Jin, and K. Zhu.

Quenching of superconductivity by Co doping in  $K_{0.8}Fe_2Se_2$ . arXiv:1102.3506, 2011.

- [174] W. Bao, Q. Huang, G. F. Chen, M. A. Green, D. M. Wang, J. B. He, X. Q. Wang, and Y. Qiu. A Novel Large Moment Antiferromagnetic Order in K<sub>0.8</sub>Fe<sub>1.6</sub>Se<sub>2</sub> Superconductor. arXiv:1102.0830, 2011.
- [175] K. Wang, H. Lei, and C. Petrovic. Thermoelectric studies of  $K_x$ Fe<sub>2-y</sub>Se<sub>2</sub>: weakly correlated superconductor without significant Fermi surface nesting. arXiv:1102.2217, 2011.
- [176] C.-H. Li, B. Shen, F. Han, X. Zhu, and H.-H. Wen. Transport properties and anisotropy of Rb<sub>0.8</sub>Fe<sub>2</sub>Se<sub>2</sub> single crystals. *arXiv:1012.5637*, 2010.
- [177] D. H. Ryan, W. N. Rowan-Weetaluktuk, J. M. Cadogan, R. Hu, W. E. Straszheim, S. L. Bud'ko, and P. C. Canfield. <sup>57</sup>Fe Mössbauer study of magnetic ordering in superconducting K<sub>0.85</sub>Fe<sub>1.83</sub>Se<sub>2.09</sub> single crystals. *arXiv:1103.0059*, 2011.
- [178] J. J. Ying, X. F. Wang, X. G. Luo, Z. Y. Li, Y. J. Yan, M. Zhang, A. F. Wang, P. Cheng, G. J. Ye, Z. J. Xiang, R. H. Liu, and X. H. Chen. Pressure effect on superconductivity of  $A_x$ Fe<sub>2</sub>Se<sub>2</sub> (A = K and Cs). arXiv:1101.1234, 2011.
- [179] Daixiang Mou, Shanyu Liu, Xiaowen Jia, Junfeng He, Yingying Peng, Lin Zhao, Li Yu, Guodong Liu, Shaolong He, Xiaoli Dong, Jun Zhang, Hangdong Wang, Chiheng Dong, Minghu Fang, Xiaoyang Wang, Qinjun Peng, Zhimin Wang, Shenjin Zhang, Feng Yang, Zuyan Xu, Chuangtian Chen, and X. J. Zhou. Distinct Fermi Surface Topology and Nodeless Superconducting Gap in (Tl<sub>0.58</sub>Rb<sub>0.42</sub>)Fe<sub>1.72</sub>Se<sub>2</sub> Superconductor. Phys. Rev. Lett., 106:107001, 2011.
- [180] J. Guo, X. Chen, G. Wang, T. Zhou, X. Lai, S. Jin, S. Wang, and K. Zhu. Superconductivity on the verge of Mott localization in ternary iron sulfide. arXiv:1102.3505, 2011.
- [181] X.-P. Wang, T. Qian, P. Richard, P. Zhang, J. Dong, H.-D. Wang, C.-H. Dong, M.-H. Fang, and H. Ding. Strong nodeless pairing on separate electron Fermi surface sheets in (Tl,K)Fe<sub>1.78</sub>Se<sub>2</sub> probed by ARPES. *Europhys. Lett.*, 93:57001, 2011.
- [182] L. Ma, G. F. Ji, J. B. He, D. M. Wang, G. F. Chen, W. Bao, and W. Yu. <sup>77</sup>Se Single Crystal NMR Study on Tl<sub>0.47</sub>Rb<sub>0.34</sub>Fe<sub>1.63</sub>Se<sub>2</sub> Superconductor. arXiv:1102.3888, 2011.
- [183] Y. Kawasaki, Y. Mizuguchi, K. Deguchi, T. Watanabe, T. Ozaki, S. Tsuda, T. Yamaguchi, H. Takeya, and Y. Takano. Pressure study of the new iron-based superconductor K<sub>0.8</sub>Fe<sub>2</sub>Se<sub>2</sub>. arXiv:1101.0896, 2011.
- [184] J. Guo, L. Sun, C. Zhang, J. Guo, X. Chen, Q. Wu, D. Gu, P. Gao, X. Dai, and Z. Zhao. Correlation between superconductivity and resistance hump in K<sub>0.8</sub>Fe<sub>1.7</sub>Se<sub>2</sub> single crystal under high pressure. *arXiv:1101.0092*, 2011.
- [185] Xun-Wang Yan, Miao Gao, Zhong-Yi Lu, and Tao Xiang. Electronic Structures

and Magnetic Order of Ordered-Fe-Vacancy Ternary Iron Selenides TlFe<sub>1.5</sub>Se<sub>2</sub> and AFe<sub>1.5</sub>Se<sub>2</sub> (A = K, Rb, or Cs). *Phys. Rev. Lett.*, 106:087005, 2011.

- [186] X.-W. Yan, M. Gao, Z.-Y. LU, and T. Xiang. Ternary iron selenide K<sub>0.8</sub>Fe<sub>1.6</sub>Se<sub>2</sub> is an antiferromagnetic semiconductor. *arXiv:1102.2215*, 2011.
- [187] I. R. Shein and A. L. Ivanovskii. Electronic structure and Fermi surface of new K intercalated iron selenide superconductor  $K_xFe_2Se_2$ . arXiv:1012.5164, 2010.
- [188] I. A. Nekrasov and M. V. Sadovskii. Electronic Structure, Topological Phase Transitions and Superconductivity in (K,Cs)xFe2Se2. *Pisma ZhETF*, 93:182, 2011.
- [189] C. Cao and J. Dai. Electronic Structure of KFe<sub>2</sub>Se<sub>2</sub> from First Principles Calculations. arXiv:1012.5621, 2010.
- [190] C. Cao and J. Dai. Electronic Structure and Mott Localization in Iron Deficient  $TlFe_{2-x}Se_2$  with Superstructures. arXiv:1101.0533, 2011.
- [191] Y. Zhang, L. X. Yang, M. Xu, Z. R. Ye, F. Chen, C. He, J. Jiang, B. P. Xie, J. J. Ying, X. F. Wang, X. H. Chen, J. P. Hu, and D. L. Feng. Nodeless superconducting gap in  $A_x$ Fe<sub>2</sub>Se<sub>2</sub> (A = K, Cs) revealed by angle-resolved photoemission spectroscopy. *Nature Mater.*, 10:273, 2010.
- [192] T. Qian, X.-P. Wang, W.-C. Jin, P. Zhang, P. Richard, G. Xu, X. Dai, Z. Fang, J.-G. Guo, X.-L. Chen, and H. Ding. Absence of holelike Fermi surface in superconducting K<sub>0.8</sub>Fe<sub>1.7</sub>Se<sub>2</sub> revealed by ARPES. arXiv:1012.6017, 2010.
- [193] L. Zhao, D. Mou, S. Liu, X. Jia, J. He, Y. Peng, L. Yu, X. Liu, G. Liu, S. He, X. Dong, J. Zhang, J. B. He, D. M. Wang, G. F. Chen, J. G. Guo, X. L. Chen, X. Wang, Q. Peng, Z. Wang, S. Zhang, F. Yang, Z. Xu, C. Chen, and X. J. Zhou. Common Fermi Surface Topology and Nodeless Superconducting Gap in K<sub>0.68</sub>Fe<sub>1.79</sub>Se<sub>2</sub> and (Tl<sub>0.45</sub>K<sub>0.34</sub>)Fe<sub>1.84</sub>Se<sub>2</sub> Superconductors Revealed from Angle-Resolved Photoemission Spectroscopy. arXiv:1102.1057, 2011.
- [194] T. A. Maier, S. Graser, P. J. Hirschfeld, and D. J. Scalapino. d-wave pairing from spin fluctuations in the  $K_xFe_{2-y}Se_2$  superconductors. arXiv:1101.4988, 2011.
- [195] I. I. Mazin and J. Schmalian. Pairing symmetry and pairing state in ferropnictides: Theoretical overview. *Physica C*, 469:614, 2009.
- [196] Fa Wang, Fan Yang, Miao Gao, Zhong-Yi Lu, Tao Xiang, and Dung-Hai Lee. The electron pairing of  $K_xFe_{2-y}Se_2$ . Europhys. Lett., 93:57003, 2011.
- [197] Y. Zhou, D.-H. Xu, W.-Q. Chen, and F.-C. Zhang. Theory for s-wave superconductivity in  $(Tl,K)Fe_xSe_2$  as a doped Mott insulator. arXiv:1101.4462, 2011.
- [198] Yi-Zhuang You, Fan Yang, Su-Peng Kou, and Zheng-Yu Weng. Phase diagram and a possible unified description of intercalated iron selenide superconductors. arXiv:1103.1902, 2011.
- [199] T. Saito, S. Onari, and H. Kontani. Emergence of Fully-Gapped  $s_{++}$ -wave and Nodal d-wave States Mediated by Orbital- and Spin-Fluctuations in Ten-Orbital Model for KFe<sub>2</sub>Se<sub>2</sub>. arXiv:1102.4049, 2011.

[200] L. Ma, J. B. He, D. M. Wang, G. F. Chen, and W. Yu. <sup>77</sup>Se NMR Evidence of Strongly Coupled Superconductivity in  $K_{0.8}Fe_{2-x}Se_2$ . arXiv:1101.3687, 2011.

- [201] Fei Han, Bing Shen, Zhen-Yu Wang, and Hai-Hu Wen. Reversibly tuning the insulating and superconducting state in  $K_xFe_{2-y}Se_2$  crystals by post-annealing. arXiv:1103.1347, 2011.
- [202] W. Bao, G. N. Li, Q. Huang, G. F. Chen, J. B. He, M. A. Green, Y. Qiu, D. M. Wang, and J. L. Luo. Vacancy tuned magnetic high- $T_c$  superconductor  $K_xFe_{2-x/2}Se_2$ . arXiv:1102.3674, 2011.
- [203] R. Yu, J.-X. Zhu, and Q. Si. Mott transition in Modulated Lattices and Parent Insulator of (K,Tl)FexSe2. arXiv:1101.3307, 2011.
- [204] Alaska Subedi, Lijun Zhang, David J. Singh, and Mao-Hua Du. Density functional study of FeS, FeSe and FeTe: Electronic structure, magnetism, phonons and superconductivity. *Phys. Rev. B*, 78:134514, 2008.
- [205] Y. Xia, D. Qian, L. Wray, D. Hsieh, G. F. Chen, J. L. Luo, N. L. Wang, and M. Z. Hasan. Fermi Surface Topology and Low-Lying Quasiparticle Dynamics of Parent Fe<sub>1+x</sub>Te/Se Superconductor. *Phys. Rev. Lett.*, 103:037002, 2009.
- [206] K. Nakayama, T. Sato, P. Richard, T. Kawahara, Y. Sekiba, T. Qian, G. F. Chen, J. L. Luo, N. L. Wang, H. Ding, and T. Takahashi. Angle-Resolved Photoemission Spectroscopy of the Iron-Chalcogenide Superconductor Fe<sub>1.03</sub>Te<sub>0.7</sub>Se<sub>0.3</sub>: Strong Coupling Behavior and the Universality of Interband Scattering. *Phys. Rev. Lett.*, 105:197001, 2010.
- [207] D. Fruchart, P. Convert, P. Wolfers, R. Madar, J. P. Senateur, and R. Fruchart. Structure antiferroma gnetique de Fe<sub>1.125</sub>Te accompagnee d'une deformation monoclinique. *Mater. Res. Bull.*, 10:169, 1975.
- [208] Alexander V. Balatsky and David Parker. Not all iron superconductors are the same. *Physics*, 2:59, 2009.
- [209] Myung Joon Han and Sergey Y. Savrasov. Doping Driven  $(\pi, 0)$  Nesting and Magnetic Properties of Fe<sub>1+x</sub>Te Superconductors. *Phys. Rev. Lett.*, 103:067001, 2009.
- [210] Fengjie Ma, Wei Ji, Jiangping Hu, Zhong-Yi Lu, and Tao Xiang. First-Principles Calculations of the Electronic Structure of Tetragonal  $\alpha$ -FeTe and  $\alpha$ -FeSe Crystals: Evidence for a Bicollinear Antiferromagnetic Order. *Phys. Rev. Lett.*, 102:177003, 2009.
- [211] Ari M. Turner, Fa Wang, and Ashvin Vishwanath. Kinetic magnetism and orbital order in iron telluride. *Phys. Rev. B*, 80:224504, 2009.
- [212] Chen Fang, B. Andrei Bernevig, and Jiangping Hu. Theory of Magnetic Order in  $Fe_{1+y}Te_{1-x}Se_x$ . Europhys. Lett., 86:67005, 2009.
- [213] Chang-Youn Moon and Hyoung Joon Choi. Chalcogen-Height Dependent Magnetic Interactions and Magnetic Order Switching in  $FeSe_xTe_{1-x}$ . Phys. Rev. Lett., 104:057003, 2010.

[214] Igor A. Zaliznyak, Zhijun Xu, John M. Tranquada, Genda Gu, Alexei M. Tsvelik, and Matthew B. Stone. Unconventional temperature enhanced magnetism in iron telluride. arXiv:1103.5073, 2011.

- [215] T. Imai, K. Ahilan, F. L. Ning, T. M. McQueen, and R. J. Cava. Why Does Undoped FeSe Become A High  $T_c$  Superconductor Under Pressure? *Phys. Rev. Lett.*, 102:177005, 2009.
- [216] M. Bendele, A. Amato, K. Conder, M. Elender, H. Keller, H.-H. Klauss, H. Luetkens, E. Pomjakushina, A. Raselli, and R. Khasanov. Pressure Induced Static Magnetic Order in Superconducting FeSe<sub>1-x</sub>. Phys. Rev. Lett., 104:087003, 2010.
- [217] H. Sabrowsky, M. Rosenberg, D. Welz, P. Deppe, and W. Schäfer. A neutron and Mösbauer study of  $TlFe_xS_2$  compounds. *J. Magn. Magn. Mater.*, 54-57:1497, 1986.
- [218] Lennart Hägström, Agneta Seidel, and Rolf Berger. A Mösbauer study of antiferromagnetic ordering in iron deficient TlFe<sub>2-x</sub>Se<sub>2</sub>. J. Magn. Magn. Mater., 98:37, 1991.
- [219] Chen Fang, Bao Xu, Pengcheng Dai, Tao Xiang, and Jiangping Hu. Magnetic Frustration and Iron-Vacancy Ordering in Iron-Chalcogenide. arXiv:1103.4599, 2011.
- [220] F. Ye, S. Chi, W. Bao, X. F. Wang, J. J. Ying, X. H. Chen, H. D. Wang, C. H. Dong, and M. Fang. Common Structural and Magnetic Framework in the A<sub>2</sub>Fe<sub>4</sub>Se<sub>5</sub> Superconductors. arXiv:1102.2882, 2011.
- [221] Z. Wang, Y. J. Song, H. L. Shi, Z.W. Wang, Z.Chen, H. F. Tian, G. F. Chen, J. G. Guo, H. X. Yang, and J. Q. Li. Microstructure and Fe-vacancy ordering in the KFe<sub>x</sub>Se<sub>2</sub> superconducting system. *arXiv:1101.2059*, 2011.
- [222] T. A. Maier and D. J. Scalapino. Theory of neutron scattering as a probe of the superconducting gap in the iron pnictides. *Phys. Rev. B*, 78:020514(R), 2008.
- [223] T. A. Maier, S. Graser, D. J. Scalapino, and P. Hirschfeld. Neutron scattering resonance and the iron-pnictide superconducting gap. *Phys. Rev. B*, 79:134520, 2009.
- [224] Eugene Demler and Shou-Cheng Zhang. Theory of the Resonant Neutron Scattering of High- $T_c$  Superconductors. *Phys. Rev. Lett.*, 75:4126, 1995.
- [225] C. D. Batista, G. Ortiz, and A. V. Balatsky. Unified description of the resonance peak and incommensuration in high- $T_c$  superconductors. *Phys. Rev. B*, 64:172508, 2001.
- [226] D. N. Argyriou, A. Hiess, A. Akbari, I. Eremin, M. M. Korshunov, Jin Hu, Bin Qian, Zhiqiang Mao, Yiming Qiu, Collin Broholm, and W. Bao. Incommensurate itinerant antiferromagnetic excitations and spin resonance in the FeTe<sub>0.6</sub>Se<sub>0.4</sub> superconductor. *Phys. Rev. B*, 81:220503, 2010.

[227] Shiliang Li, Chenglin Zhang, Meng Wang, Hui-qian Luo, Xingye Lu, Enrico Faulhaber, Astrid Schneidewind, Peter Link, Jiangping Hu, Tao Xiang, and Pengcheng Dai. Normal-State Hourglass Dispersion of the Spin Excitations in FeSe<sub>x</sub>Te<sub>1-x</sub>. Phys. Rev. Lett., 105:157002, 2010.

- [228] P. Babkevich, M. Bendele, A. T. Boothroyd, K. Conder, S. N. Gvasaliya, R. Khasanov, E. Pomjakushina, and B. Roessli. Magnetic excitations of  $\text{Fe}_{1+y}\text{Se}_x\text{Te}_{1-x}$  in magnetic and superconductive phases. *J. Phys. Conden. Matter*, 22:142202, 2010.
- [229] M. D. Lumsden, A. D. Christianson, E. A. Goremychkin, S. E. Nagler, H. A. Mook, M. B. Stone, D. L. Abernathy, T. Guidi, G. J. MacDougall, C. De La Cruz, A. S. Sefat, M. A. McGuire, B. C. Sales, and D. Mandrus. Evolution of spin excitations into the superconducting state in FeTe<sub>1-x</sub>Se<sub>x</sub>. Nature Phys., 6:182, 2010.
- [230] S. O. Diallo, V. P. Antropov, T. G. Perring, C. Broholm, J. J. Pulikkotil, N. Ni, S. L. Bud'ko, P. C. Canfield, A. Kreyssig, A. I. Goldman, and R. J. McQueeney. Itinerant Magnetic Excitations in Antiferromagnetic CaFe<sub>2</sub>As<sub>2</sub>. *Phys. Rev. Lett.*, 102:187206, 2009.
- [231] Jun Zhao, D. T. Adroja, Dao-Xin Yao, R. Bewley, Shiliang Li, X. F. Wang, G. Wu, X. H. Chen, Jiangping Hu, and Pengcheng Dai. Spin Waves and Magnetic Exchange Interactions in CaFe<sub>2</sub>As<sub>2</sub>. Nature Phys., 5:555, 2009.
- [232] P. Dai, H. A. Mook, G. Aeppli, S. M. Hayden, F. Doğan, J. Yu, Y. Yanagida, H. Takashima, Y. Inaguma, M. Itoh, and T. Nakamura. Resonance as a measure of pairing correlations in the high- $T_c$  superconductor YBCO. *Nature*, 406:965, 2000.
- [233] J. M. Tranquada, C. H. Lee, K. Yamada, Y. S. Lee, L. P. Regnault, and H. M. Rønnow. Evidence for an incommensurate magnetic resonance in  $La_{2-x}Sr_xCuO_4$ . *Phys. Rev. B*, 69:174507, 2004.
- [234] Jun Zhao, Louis-Pierre Regnault, Chenglin Zhang, Miaoying Wang, Zhengcai Li, Fang Zhou, Zhongxian Zhao, Chen Fang, Jiangping Hu, and Pengcheng Dai. Neutron spin resonance as a probe of the superconducting energy gap of BaFe<sub>1.9</sub>Ni<sub>0.1</sub>As<sub>2</sub> superconductors. *Phys. Rev. B*, 81:180505, 2010.
- [235] Ph. Bourges, B. Keimer, S. Pailhòes, L.P. Regnault, Y. Sidis, and C. Ulrich. The resonant magnetic mode: A common feature of high-Tc superconductors. *Physica C*, 424:45, 2005.
- [236] Wei Bao, A. T. Savici, G. E. Granroth, C. Broholm, K. Habicht, Y. Qiu, Jin Hu, Tijiang Liu, and Z. Q. Mao. A Triplet Resonance in Superconducting FeSe<sub>0.4</sub>Te<sub>0.6</sub>. arXiv:1002.1617, 2010.
- [237] Wei-Guo Yin, Chi-Cheng Lee, and Wei Ku. Unified Picture for Magnetic Correlations in Iron-Based Superconductors. *Phys. Rev. Lett.*, 105:107004, 2010.

[238] O. J. Lipscombe, G. F. Chen, Chen Fang, T. G. Perring, D. L. Abernathy, A. D. Christianson, Takeshi Egami, Nanlin Wang, Jiangping Hu, and Pengcheng Dai. Spin Waves in the  $(\pi,0)$  Magnetically Ordered Iron Chalcogenide Fe<sub>1.05</sub>Te. *Phys. Rev. Lett.*, 106:057004, 2011.

- [239] C. Stock, E. E. Rodriguez, M. A. Green, and J. A. Rodriguez-Rivera. Gapped spin fluctuations and interstitial iron in the  $Fe_{1+x}$ Te parent compound. arXiv:1103.1347, 2011.
- [240] Z. Xu, J. Wen, G. Xu, S. Chi, W. Ku, G. Gu, and J. M. Tranquada. Evidence for local moment magnetism in superconducting FeTe<sub>0.35</sub>Se<sub>0.65</sub>. arXiv:1012.2300, 2010.